

# Toward Deterministic Satellite-Terrestrial Integrated Networks via Resource Adaptation and Differentiated Scheduling

Weiting Zhang<sup>ID</sup>, Member, IEEE, Peixi Liao<sup>ID</sup>, Dong Yang<sup>ID</sup>, Member, IEEE, Qiang Ye<sup>ID</sup>, Senior Member, IEEE, Shiwen Mao<sup>ID</sup>, Fellow, IEEE, and Hongke Zhang<sup>ID</sup>, Fellow, IEEE

**Abstract**—Satellite-terrestrial integrated network (STIN) is a full-scale communication paradigm, which can support joint information processing and seamless service provision by leveraging satellites' wide coverage and terrestrial networks' high capacity. The existing STIN operates with insufficient synergy in transmission scheduling, impacting resource allocation efficiency and transmission delay optimization, particularly in complex transmission scenarios. In this paper, we design Deterministic STIN (DetSTIN), a novel architecture for STIN, along with two algorithms tailored for transmission scheduling to collaboratively optimize resource adaptation and service flow scheduling. Specifically, the DetSTIN enables the smooth interconnection and integration of heterogeneous networks by providing layered deterministic services. Besides, a genetic-based resource adaptation algorithm is designed for fixed-mobile-satellite heterogeneous networks to reduce resource allocation overhead while maintaining the network performance. Furthermore, we propose a deep reinforcement learning-based differentiated scheduling algorithm to solve the routing-queue two-dimensional decision problem to differentially optimize transmission delay of service flows, thus obtaining higher transmission scheduling benefit. By addressing resource adaptation and differentiated scheduling synergistically, the proposed solution achieves reduced resource allocation overhead and increased transmission scheduling benefit, ultimately leading to increased network operation revenue of the DetSTIN. Simulation results demonstrate that the proposed solution delivers effective performance across various flow proportions, and as the number of flows increases, the network operation revenue exhibits a noticeable improvement, compared with benchmark algorithms.

**Index Terms**—Satellite-terrestrial integrated networks, resource adaptation, differentiated scheduling, deep reinforcement learning.

Received 27 December 2024; revised 30 April 2025; accepted 21 May 2025. Date of publication 28 May 2025; date of current version 3 September 2025. This work was supported by the National Natural Science Foundation of China under Grant 62425104 and Grant 62394321. An earlier version of this paper was presented at the IEEE/CIC ICCC 2024 [DOI: 10.1109/ICCC62479.2024.10682000]. Recommended for acceptance by H. Hu. (Corresponding author: Dong Yang.)

Weiting Zhang, Peixi Liao, Dong Yang, and Hongke Zhang are with the School of Electronic and Information Engineering, Beijing Jiaotong University, Beijing 100044, China (e-mail: wtzhang@bjtu.edu.cn; pxliao@bjtu.edu.cn; dyang@bjtu.edu.cn; hkzhang@bjtu.edu.cn).

Qiang Ye is with the Department of Electrical and Software Engineering, Schulich School of Engineering, University of Calgary, Calgary, AB T2N 1N4, Canada (e-mail: qiang.ye@ucalgary.ca).

Shiwen Mao is with the Department of Electrical and Computer Engineering, Auburn University, Auburn, AL 36849-5201 USA (e-mail: smao@ieee.org).

Digital Object Identifier 10.1109/TMC.2025.3574740

## I. INTRODUCTION

**I**N RECENT years, massive terminal access has spurred the rapid development and large-scale deployment of fifth-generation (5G) networks [2], [3]. Meanwhile, the focus of network functions has shifted from merely ensuring reliable transmission to delivering *differentiated* and *customizable* services, thus creating an urgent demand for geographically extensive coverage and transmission guarantees by design [4]. However, existing terrestrial mobile communication systems are constrained by limited coverage. With the vision of ubiquitous connectivity and heterogeneous network convergence in sixth-generation (6G) [5], [6], satellite-terrestrial integrated networks (STIN) have emerged as a promising solution due to their capacity to provide ubiquitous, consistent, and scalable services [7]. Serving as a complement to terrestrial networks, satellite networks can provide seamless communication access to global users, effectively mitigating coverage gaps [8]. The STIN is not merely a simple interconnection between satellite and terrestrial networks. Conversely, it represents a full-scale integration of heterogeneous networks at the architectural level [9].

As STIN transitions from basic compatibility in 5G to full-scale integration in 6G, significant advancements have been made in various domains to address the challenges posed by the STIN [10], [11], [12], [13], [14]. From a network management perspective, Yao et al. introduced a novel heterogeneous wireless network architecture, named SI-STIN, based on the concept of a Smart Identifier Network, which aims to address the issue of heterogeneous integration at the network layer within the STIN [15]. However, there are deficiencies in supporting network automation functions. In terms of architectural design, Eiza et al. designed a hybrid software-defined networking (SDN)-based architecture for secure and quality of service (QoS)-aware routing in the STIN, employing multiple SDN controllers operating at different hierarchies [16]. From a resource allocation perspective, Hurmat et al. addressed the challenge of network control and resource allocation for massive Internet of Things (IoT) deployments in the STIN by developing a hierarchical actor-critic network-based solution [17]. Although existing researches have made progress in network management, architectural design, and resource allocation, there remains a lack of a generally applicable resource allocation algorithm to effectively support the heterogeneous integration and large-scale

deployment of the STIN [18], [19], [20], [21], [22]. Current approaches generally focus on specific scenarios or requirements, making it difficult for them to be widely applicable in diverse network environments.

Simultaneously, the aggregation of massive services has imposed higher demands on the effectiveness and efficiency of the integrated networks [23], [24], [25]. There is a growing demand from users for transmission reliability [26], [27]. In response, deterministic technologies, such as time-sensitive networking (TSN) for LANs, deterministic networking (DetNet) and deterministic IP (DIP) for WANs, and 5G-TSN for fixed-mobile combined scenarios, have been arisen as research focuses [27], [28], [29]. These technologies provide strong service guarantees, offering deterministic delay and predictable QoS through mechanisms such as explicit routing, congestion control, queuing, shaping, and scheduling algorithms [30], [31]. From TSN focusing on traffic shaping and DetNet considering multi-queue scheduling [32] to cross-domain mapping of large-scale deterministic networks, deterministic technologies have been widely explored [33]. In the literature, there exist a line of works investigating deterministic transmission scheduling, which focus on terrestrial or satellite networks. Zhang et al. proposed an incremental scheduling algorithm based on traffic judgment conditions and position diversity search boundaries to reduce scheduling complexity while maintaining a mixed transmission of periodic and non-periodic flows for load balancing [34]. Yang et al. adopted a mechanism combining TSN and cyclic queuing and forwarding (CQF) for facilitating efficient deterministic federated learning [35]. A redundant encoding and multi-path scheduling algorithm is proposed, which leverages ephemeris information and dynamic resource update mechanisms to construct deterministic spatio-temporal routing paths [36]. Li et al. proposed a joint routing and scheduling algorithm based on segment routing, including end-to-end (E2E) delay prediction, probabilistic packet dropping, and cyclic specified queuing and forwarding (CSQF) modules [37]. Peng et al. proposed a deterministic cross-domain flow scheduling solution to address the challenges posed by inter-domain microbursts, which are not adequately considered in TSN and DetNet [38].

Deterministic STIN (DetSTIN) combining deterministic technologies with the STIN appears to be a promising solution for achieving deterministic transmission scheduling in wide-coverage network scenarios and delivering customized communication services to users. However, since the deterministic technologies and STIN are still in the nascent stage, there is an urgent need to investigate how to achieve deep integration from architectural and mechanistic perspectives. Wang et al. proposed a general scheduling model that maps time-triggered (TT) flows to the underlying low-earth-orbit (LEO) resources of STINs and introduced a cyclic priority and forwarding mechanism to improve the performance of time-sensitive services [39]. However, this scheme does not take non-TT flows into account, thereby limiting its applicability across a wider range of operational scenarios. Yu et al. envisioned a DetNet-enabled non-terrestrial network architecture and designed a deterministic network selection and routing scheme to guarantee E2E delay of holographic flows [40]. However, there remains a paucity

of effective deterministic resource allocation and transmission scheduling schemes for the DetSTIN.

In fact, addressing deterministic transmission scheduling issues in the DetSTIN faces significant challenges. On one hand, satellite networks, particularly LEO satellites, exhibit dynamic network topologies due to the inherent mobility of satellites [41]. This mobility leads to frequent changes in communication links, which complicates resource allocation and makes it difficult to ensure resource stability and continuity. Therefore, designing a simple yet efficient resource allocation algorithm that can adapt to the dynamic essence of satellite networks and guarantee deterministic resource utilization is crucial. On the other hand, the dynamic and unpredictable essence of transmission paths in satellite networks further exacerbates the complexity of transmission scheduling, and how to optimize transmission scheduling through cross-domain collaboration to ensure E2E QoS becomes a problem [3]. Since satellite and terrestrial networks have been developed and operated independently [42], existing deterministic transmission scheduling mechanisms designed for terrestrial networks cannot be directly applied to satellite networks without substantial modifications. Therefore, there is a pressing need for a flexible scheduling algorithm that can not only accommodate the dynamic topologies but also ensure deterministic transmission within the DetSTIN.

To address the above challenges, this paper investigates two problems: (1) the optimization of network performance through deterministic resource adaptation, focusing on minimizing resource allocation overhead while maintaining overall network efficiency; and (2) the enhancement of transmission scheduling performance via differentiated scheduling, aiming to optimize transmission scheduling benefit while ensuring users' QoS. In our previous work of [1], we briefly introduce the Transient Routing And Varied quEue aLgorithm (TRAVEL) to improve transmission scheduling performance and benefit. In this paper, we extend our previous work and consider the impact of resource adaptation on network performance and overhead, further improving network operation revenue. The main contributions of this paper can be summarized as follows:

- We propose a DetSTIN architecture that seamlessly integrates the entity domain with deterministic technical support. This architecture enables the smooth interconnection and integration of heterogeneous networks by providing layered deterministic services. It ensures consistent communication, efficient resource utilization, and reliable transmission across diverse network environments.
- We formulate a joint resource allocation and transmission scheduling problem to maximize network operation revenue while satisfying QoS requirements. This problem takes into account the limited resources with different unit configuration overhead of the DetSTIN and guarantees that service flows obtain the requisite resources and satisfactory delay for efficient transmission.
- We decouple the problem into two interrelated subproblems and address them separately. For resource allocation, we design an improved genetic-based algorithm to optimize intra-domain resource allocation while maintaining network performance. For transmission scheduling, we

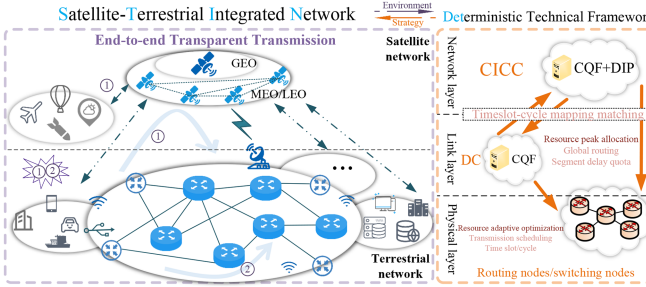


Fig. 1. DetSTIN architecture.

propose a deep reinforcement learning (RL)-based algorithm to dynamically schedule service flows based on the allocated resources.

The remainder of this paper is structured as follows: The system model and the problem formulation are presented in Sections II and III, respectively. Section IV elaborates on the proposed algorithms. Subsequently, we show the simulation results of the solution in Section V, and give conclusions and discussions in Section VI.

## II. SYSTEM MODEL

### A. Network Model

As illustrated in Fig. 1, the architecture of the DetSTIN ensures E2E high-reliability and low-delay transmission by employing a deterministic technical framework. This framework plays a critical role in ensuring E2E deterministic performance through multi-layer collaboration across the network, data link, and physical layers. The core of this framework is the centralized intelligent control center (CICC), which oversees global timeslot-cycle mapping, determines peak resource allocation, and formulates global routing decisions. Besides, the CICC operates in conjunction with domain controllers (DC) within each domain. Based on the above routing decisions, segment delay quotas are assigned to each domain and cross-domain link. DC dynamically optimizes peak resource allocation and is responsible for intra-domain differentiated scheduling according to the corresponding delay quota, maintaining deterministic flow transmission within their respective domains. This multi-layered collaborative mode not only optimizes resource allocation but also ensures deterministic transmission across different domains, thereby guaranteeing high-quality service delivery throughout the DetSTIN.

Within the entity network, *fixed-mobile terminals* encompass a wide range of devices, such as industrial gateways in fixed scenarios and vehicle-mounted radars in mobile scenarios. These terminals are equipped with dual-mode communication chips, enabling seamless switching between terrestrial and satellite networks. This capability ensures efficient and accurate forwarding of service flows, either through terrestrial networks or through inter-satellite links. For communication in the DetSTIN, the “CQF+DIP” paradigm is employed to ensure long-distance deterministic transmission. Specifically, in

satellite-based delay-tolerant network scenarios, laser technologies are deployed in both satellite-terrestrial and inter-satellite communications, while optical fiber technology is employed for terrestrial communication [43], [44]. Laser-based and optical fiber-based communication present multiple crucial advantages, such as high transmission rates and robust interference resistance capabilities.

The *terrestrial networks* comprise ground communication networks, gateway stations, and the CICC. Gateway stations are responsible for establishing laser communication links with the satellite networks, facilitating efficient data exchange between terrestrial and satellite networks. In parallel, the CICC serves as the global control and management center for the DetSTIN to support deterministic transmission scheduling and deliver high-quality services between satellite and terrestrial. Additionally, the *time-varying satellite networks* integrate geostationary earth orbit (GEO), medium earth orbit (MEO), and LEO satellites, governed by intelligent control principles. GEO satellites, equipped with advanced on-satellite monitoring and control capabilities, act as logical sub-controllers. These satellites receive peak resource allocation and global routing decisions from the CICC, which are converted into control commands and then distributed to MEO and LEO satellites [45], [46]. MEO and LEO satellites execute deterministic forwarding of service flows via highly reliable inter-satellite laser links, enabling seamless and efficient flow transmission across the satellite networks.

For concretized description, the DetSTIN is modeled as an undirected graph  $G(V, \mathcal{E})$ , where the sets of nodes and links are denoted by  $V = \{v_0, v_1, \dots, v_n\}$  and  $\mathcal{E} = \{e \mid e_{kj} = (v_k, v_j), e_{jl} = (v_j, v_l), \dots\}$ , respectively. The set of service flows generated by terminals is denoted by

$$\mathcal{F} = \{f \mid f_i = \langle v_{f_i}^{sou}, v_{f_i}^{des}, C_{f_i}, D_{f_i}, \xi_{f_i}, \rangle, \forall i \in [1, |\mathcal{F}|]\}, \quad (1)$$

where  $f_i$  denotes the  $i$ -th service flow in the flow set with length  $|\mathcal{F}|$ , and  $v_{f_i}^{sou}$  and  $v_{f_i}^{des}$  are the source and destination nodes, respectively. Additionally,  $C_{f_i}$  and  $D_{f_i}$  are the size and delay requirement, and  $\xi_{f_i}$  is the unit benefit for E2E delay optimization. Based on the delay requirements, service flows can be classified into three categories: TT, audio video bridging (AVB), and best-effort (BE) flows.

### B. Deterministic Technical Framework

To achieve efficient and reliable service flow transmission within the DetSTIN, as shown in Fig. 2, we propose a resource adaptation module and subsequently design a differentiated scheduling module leveraging deterministic technologies, in which the latter's decision is built upon the outcome of the former, ensuring an integrated solution between resource allocation and differentiated scheduling, thereby improving overall transmission determinism and efficiency.

*1) Resource adaptation:* Resource adaptation is to ensure sufficient capacity for the cache of service flows at nodes, comprising two core components: inter-domain peak cache resource reservation driven by the CICC and intra-domain adaptive cache optimization managed by the DC [47]. From a global perspective, the CICC analyzes the characteristics of service flows and

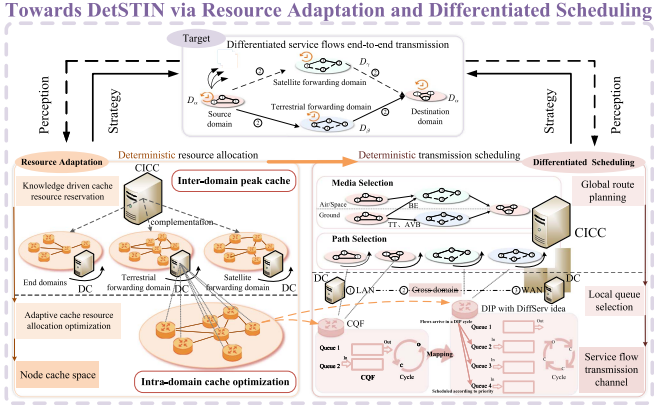


Fig. 2. DetSTIN supported by resource adaptation and differentiated scheduling modules.

historical data across domains to reasonably predict and reserve peak cache resources, ensuring stability and sufficiency during inter-domain transmission. Meanwhile, the DC is responsible for dynamically adjusting the cache resource allocation based on real-time network conditions and flow variations within the domain, thereby achieving efficient resource utilization and rapid adaptation.

Within this module, nodes in the end domain are allocated sufficient cache resources by the CICC and DC to fully cover the cache requirements of service flows, ensuring data reliability and integrity during E2E transmission. Resources between terrestrial forwarding domain and satellite forwarding domain are allocated in a complementary manner by the CICC to collaboratively support the E2E transmission of various service flows [48]. Besides, nodes in a forwarding domain are also allocated complementarily by their associated DC to jointly complete multi-path transmission of flows. This complementary design of resource allocation not only improves network resilience but also effectively mitigates the impact of network congestion.

2) *Differentiated scheduling*: To enhance the reliability of service flow transmission and satisfy differentiated QoS requirements, this module employs global route planning determined by the CICC, which pre-allocates an E2E transmission path for each service flow. Simultaneously, the DC makes intra-domain forwarding cycle decisions by differentiating injecting service flows into appropriate queues based on their delay requirements. Proper route planning can reduce unnecessary node hops, thereby reducing overall delay [49]. Meanwhile, fine-grained queue selection enables efficient utilization of reserved cache resources, flexibly accommodating mixed service flows and improving the determinism and predictability of E2E transmission. The overview of the decision-making process is as follows:

*Global route planning*: When mixed service flows are injected into the DetSTIN, the forwarding media is first selected by the CICC, which can be represented by  $m_{f_i} \in \{0, 1\}, \forall f_i \in \mathcal{F}$ . For differentiated scheduling, TT flows, which typically have stringent delay and reliability requirements, are scheduled over shorter paths. Conversely, BE flows with more relaxed delay

requirements can be routed through longer paths. Specifically, service flows generated by aerial monitoring tasks and BE flows originating from terrestrial sources can be forwarded through satellites, denoted as  $m_{f_i} = 1$ , while other terrestrial flows are forwarded through terrestrial nodes, denoted as  $m_{f_i} = 0$ , thus offering flexibility in balancing network loads and optimizing resource utilization.

Subsequently, the CICC performs intra-domain path selection after the DC of each domain reports the feasible path within the domain. The complete transmission path for service flow  $f_i$  may be  $p_f = (v_0, v_1, \dots, v_{|p_f|})$ , where path segments  $(v_0, v_1, \dots, v_\lambda)$  and  $(v_{\mu+1}, \dots, v_{|p_f|})$  in end domains  $D_\alpha$  are usually fixed, while path segment  $(v_{\lambda+1}, v_{\lambda+2}, \dots, v_\mu)$  within terrestrial forwarding domain  $D_\beta$  or satellite forwarding domain  $D_\gamma$  offers flexible multiple options, thus constructing a globally deterministic E2E transmission path via segment path determinism. Here,  $\lambda \in (0, |p_f|)$  and  $\mu \in (0, |p_f|)$  denote node indexes. Then, segment delay quotas are assigned to domains and inter-domain links according to the path selection results.

*Local queue selection*: With the DC, service flows are forwarded periodically at each node, essentially utilizing a time-sliced queue management approach. In the end domain, the CQF mechanism with precise time synchronization is employed, using two queues that periodically switch between sending and receiving states to alternately send service flows to avoid queue congestion and uncertain delay. The critical decision lies in determining whether the service flow should be dispatched in the current cycle or deferred to the next.

In the forwarding domain, where massive amounts of heterogeneous service flows are aggregated, a mechanism that combines the concept of differentiated service (DiffServ) and DIP is employed. DiffServ is reflected on network nodes, for non-aggregation nodes with low node degrees, traditional DIP with one queue for sending and three queues for receiving is adopted; while for aggregation nodes with high node degrees, DIP with differentiated scheduling is adopted and scheduling decisions vary with different flow types.

We develop this mechanism based on following considerations: On the one hand, based on the DIP, compared with the entire per-queue scheduling of CSQF, this mechanism can achieve highly flexible per-flow scheduling and efficiently utilize the periodic cache of nodes. With this mechanism, fine-grained processing of each service flow can be realized, fully exploiting the potential of node cache resources and improving resource utilization efficiency. On the other hand, this mechanism adopts differentiated scheduling. Considering the specific scenarios that are not properly addressed by DIP, that is, when two upstream nodes send service flows to the same downstream node in the same cycle and the link delay difference is within one DIP cycle, the flows are mapped to the same cycle of the downstream node. In such a case, it is possible that BE flows arrive at the downstream node first, and then TT flows arrive. According to the DIP rules, BE flows are queued before TT flows for cache and forwarding. However, a circumstance might arise in which the cache capacity of the downstream node is insufficient. Consequently, only BE flows can be cached, and TT flows are compelled to be deferred to the subsequent cycle for forwarding.

This will inevitably increase the transmission delay of the TT flows. In response to this problem, the proposed mechanism schedules these flows according to the priority, ensuring that among the flows mapped to the same cycle, TT flows take precedence over AVB flows, and AVB flows take precedence over BE flows, so as to achieve refined flow differentiated scheduling and effectively guarantee the transmission performance and QoS requirements of different flow types.

This mechanism introduces three key enhancements to address the challenges of scheduling for the aggregated service flows. *First*, the traditional timeslot-based absolute queue scheduling is transformed into cycle-based relative queue scheduling. This eliminates the dependency on high-precision clock synchronization among nodes and allows upstream and downstream nodes to operate with misaligned cycle timings. With the DC, service flows are dynamically enqueued into relative queues based on their waiting delay requirements [50]. *Second*, different types of service flows are assigned to relative queues with specific delay based on per-hop cycle shifts, achieving temporal isolation according to their waiting delay. Different from the entire queue per-hop offset of CSQF and the per-flow offset at the gateway nodes of DIP, the proposed mechanism employs a differentiated offset with upper limit, measured by  $\psi \in \{1, 2, 3\}$ . Since the link delay of a service flow between adjacent nodes may not be integer multiples of the cycle period, we consider enqueue delay as a part of the total queue waiting delay. During the initial scheduling at nodes with high node degree, the TT flow enters the relative queue with a maximum waiting time of one DIP cycle without offset, which ensures the stability and low-delay characteristics of the TT flow transmission. For the AVB flow, it can enter the relative queues with the maximum waiting time of either one DIP cycle or two DIP cycles. While ensuring a certain transmission efficiency, it is endowed with relatively flexible scheduling space and can be adaptively scheduled according to the real-time network conditions to balance its resource occupation and transmission timeliness. For the BE flow, it is arranged to enter the relative queues with the maximum waiting time of either two DIP cycles or three DIP cycles, thus the BE flow is allowed to conduct transmission scheduling within relatively loose time limits. This differentiated scheduling ensures that high-priority flows experience minimal delays while maintaining flexibility for lower-priority flows (i.e., AVB and BE) and ensuring BE flows an equitable opportunity for forwarding and preventing BE flows from starving. The core of this mechanism is the design of relative queues, which define logical waiting times for different service flow types. Importantly, these relative queues are not directly mapped to physical queues. Instead, the DC dynamically handles this mapping based on current network conditions, queue loads, and flow priorities. This adaptive mapping ensures that, even under cycle misalignment, service flows can be forwarded within their allowable delay requirements. By abstracting the scheduling process through relative queues, the DC decouples logical flow management from physical node queues, enhancing robustness and flexibility.

*Finally*, a compensatory policy is integrated to handle exceptional cases. Within the acceptable delay, service flows that fail to be scheduled according to initial decisions or arrive prematurely

due to upstream gate control failures can be rescheduled to a relatively suboptimal queue, subject to an additional delay penalty. This ensures that even in the presence of scheduling deviations, the DC maintains a degree of flexibility to handle unexpected conditions while minimizing transmission disruptions. Notably, the rescheduling process still considers both the priority of the service flow and the current load conditions of the available queues, ensuring that high-priority service flows experience minimal impact.

In our design, the CQF and DIP mechanisms employ different numbers of gating queues  $\delta(v_j)$ , which are defined as

$$\delta(v_j) = \begin{cases} 2, & v_j \in D_\alpha, \\ 4, & v_j \in D_\beta \cup D_\gamma. \end{cases} \quad (2)$$

Given this queue configuration, cycle durations  $T_{v_j}$  are set accordingly to maintain send-receive alignment between the two mechanisms. Specifically, cycle duration in  $D_\alpha$  is two times than that in  $D_\beta$  or  $D_\gamma$ . This proportionality ensures that service flows in a CQF cycle can be fully forwarded within one DIP cycle, thereby guaranteeing the determinism of service flow transmission and achieving seamless inter-domain coordination. With the above considerations, the DetSTIN not only provides precise QoS guarantees but also demonstrates strong adaptability to dynamic network topologies and diverse traffic patterns.

### C. Service Flow Delay Model

Realizing E2E bounded delay is not only the primary objective of deterministic transmission scheduling, but also a critical metric for evaluating its efficiency. When a service flow is successfully transmitted to the destination within its delay requirement, the time saved relative to the delay requirement is referred to as the delay optimization. For service flows within a time slice, the delay optimization of different service flows bring different transmission scheduling benefit. Therefore, a comprehensive analysis of the constituents of E2E delay is indispensable for guaranteeing effective optimization of overall delay.

In accordance with the large-scale global route planning and small-scale local queue selection, for a given flow  $f_i$ , E2E delay consists of link delay and node delay accordingly, which can be expressed as

$$\mathcal{D}_i = \sum_{(v_k, v_j) \in l} \mathcal{D}_i^{e_{kj}} + \sum_{v_k, v_j \in p_{f_i}} \mathcal{D}_i^{v_j}. \quad (3)$$

Here,  $l$  represents the selected E2E path, consisting of multiple directed arcs  $e_{kj}$ , where each arc connects two adjacent nodes  $v_k$  and  $v_j$  along the path, and  $p_{f_i}$  denotes the set of nodes along the path. This equation directly reflects how the hierarchical scheduling decisions at different scales affect on the overall E2E delay.

1) *Link delay*: Link delay is equivalent to propagation delay, which can be calculated by link length and propagation speed, i.e.,  $\mathcal{D}_i^{e_{kj}} = \sum_{e_{kj}} \mathcal{L}_{e_{kj}} / \mathcal{V}_{e_{kj}}$ , where  $\mathcal{L}_{e_{kj}}$  represents the length of  $e_{kj}$  and  $\mathcal{V}_{e_{kj}}$  is propagation speed. Different propagation media has different propagation speed, which can be denoted as

$$\mathcal{V}_{e_{kj}} = \begin{cases} \mathcal{V}_s, & m_{f_i} = 1, \\ \mathcal{V}_t, & m_{f_i} = 0. \end{cases} \quad (4)$$

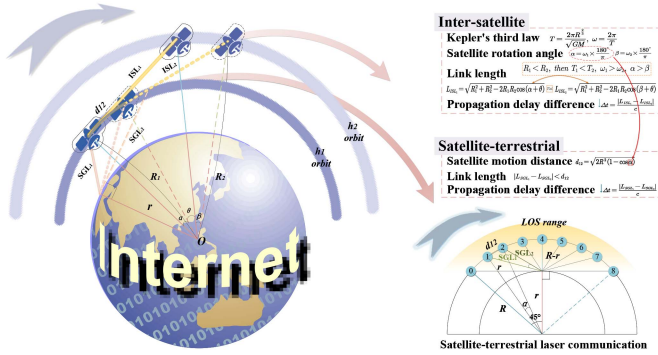


Fig. 3. Negligible impact of satellite mobility on link delay.

In the DetSTIN, it is noteworthy that despite the frequent alterations in the connection between a LEO satellite and its neighbors during their orbital traversals, significant delay jitter would not be introduced into the communication links. Note that satellites positioned around 1,000 km above the Earth's surface possess a linear velocity of about 7.5 km/s and an angular velocity of approximately  $240^\circ/\text{h}$ . Specifically, the transmission delay between a satellite and a terrestrial station amounts to approximately 3 ms. During this time interval, circular-orbit satellites such as Iridium and Teledesic experience a rotation of approximately  $0.0002^\circ$  and a displacement of around 22.5 m. This indicates that the delay jitter is negligible at the nanosecond scale, thereby effectively alleviating concerns regarding the impact of satellite mobility on link delay variability. As illustrated in Fig. 3, geometric principles further corroborate this conclusion. For inter-satellite communication, the cosine theorem verifies that the variations in communication distance attributable to satellite mobility are insignificant. Similarly, for satellite-terrestrial communication, the triangle inequality demonstrates that the alterations in propagation distance are insignificant. Consequently, the resulting changes in propagation delay are trifling. On this basis, the CICC is capable of prognostically assessing the potential delay modifications in diverse stages or links during the satellite movement process by analyzing the historical data of satellite motion and the characteristics of communication links, and subsequently allocating appropriate segment delay quotas for domains and cross-domain links in advance. During transmission process, DC can dynamically adjust the delay quotas among nodes based on the real-time satellite movement and actual delay feedback. This not only helps to distribute the delay induced by satellite movement but also enhances the reliability of the transmission process.

2) *Node delay*: Delay for flow  $f_i$  at node  $v_j$  consists of three components: transmission delay  $\mathcal{D}_{i,tr}^{v_j}$ , queuing delay  $\mathcal{D}_{i,qu}^{v_j}$ , and waiting delay  $\mathcal{D}_{i,wa}^{v_j}$ . Thus, we have

$$\mathcal{D}_i^{v_j} = \mathcal{D}_{i,tr}^{v_j} + \mathcal{D}_{i,qu}^{v_j} + \mathcal{D}_{i,wa}^{v_j}. \quad (5)$$

Here, transmission delay is defined as  $\mathcal{D}_{i,tr}^{v_j} = C_{f_i}/B_{e_{jl}}$ , where  $B_{e_{jl}}$  represents the bandwidth of outgoing link  $e_{jl}$  from node  $v_j$ . Queuing delay is given by  $\mathcal{D}_{i,qu}^{v_j} = \sum_{f_j} \mathcal{D}_{i,tr}^{v_j}$ , where  $f_j$  denotes the service flows preceding  $f_i$  in the queue. Given

the high bandwidth of laser and fiber-optic communication, both transmission delay and queuing delay can approach the nanosecond scale.

In addition, waiting delay  $\mathcal{D}_{i,wa}^{v_j}$  is related to the intrinsic gating duration of DIP cycle, which can be expressed as

$$\mathcal{D}_{i,wa}^{v_j} = (\psi_i - (\mathcal{D}_i^{e_{kj}} \bmod T_{v_j})) \cdot T_{v_j}, \quad (6)$$

where  $\psi_i$  represents the allocated queue for service flow  $f_i$ , and  $\mathcal{D}_i^{e_{kj}}$  is the link delay along  $e_{kj}$ . The waiting delay ensures that service flows are forwarded in distinct time slots, isolating different flows temporally, thus achieving fine-grained forwarding.

Specifically, the CQF mechanism operating at end domains leverages time synchronization and periodic scheduling to ensure deterministic transmission, while implicitly accounting for link delay within its cycle. Consequently, the transmission delay of  $f_i$  in the end domains can be simplified as

$$\sum_{v_j \in D_\alpha} (\lambda + |p_{f_i}| - \mu) \cdot T_{v_j}. \quad (7)$$

However, the DIP mechanism operates with finer granularity and requires real-time adjustments to accommodate dynamic link conditions. This necessitates explicit consideration of both link delay and node delay to ensure accurate scheduling.

#### D. Network Operation Revenue Model

In the DetSTIN, the efficient operation of the network depends on effective resource adaptation and differentiated scheduling. These two modules jointly determine the overall network operation revenue  $\mathcal{R}$ , which is defined as the difference between transmission scheduling benefit  $\mathcal{B}$  and resource allocation overhead  $\mathcal{OH}$ , i.e.,

$$\mathcal{R} = \mathcal{B} - \mathcal{OH}. \quad (8)$$

This relationship emphasizes the delicate balance required to optimize network performance. On one hand, transmission scheduling benefit  $\mathcal{B}$  represents the gains derived from efficient route planning and queue selection of service flows, which directly contributes to the network's ability to satisfy users' requirements and maximize throughput. On the other hand, resource allocation overhead  $\mathcal{OH}$  reflects the costs associated with managing and configuring resources across the network. Obtaining an optimal balance between these two components is essential for maximizing overall network operation revenue  $\mathcal{R}$ . Below, we detail the two components and their relationships with the network operation revenue.

1) *Resource allocation overhead*: The goal of resource allocation is to minimize resource allocation overhead while maintaining network performance (i.e., throughput rate and resource utilization). The resource allocation overhead is mainly determined by two parts: inter-domain peak cache and intra-domain cache optimization.

During time slice transitions, the CICC handles cross-domain peak cache resource allocation, while each DC independently optimizes node cache resources. Different cache resource allocation schemes have different resource allocation overhead. Specifically, the sum of the product of the peak cache size

between domains and the unit configuration overhead of each domain determines the upper limit of resource allocation overhead. This upper limit provides a basic constraint for resource allocation. Meanwhile, with the intra-domain cache optimization, resource allocation in each domain gradually tends to achieve the given throughput and resource utilization of the network with fewer resources. We assume that all service flows are indivisible, namely, they are not partitioned for transmission via multiple paths, and the resources allocated by node  $v_j$  to service flow  $f_i$  should not be smaller than the required amount. Taking queue resource  $C_{v_j}$  as an example, we have the capacity constraint, i.e.,

$$C_{v_j} \times \Phi_i \geq C_{f_i}, \quad \forall f_i \in \mathcal{F}, v_j \in p_{f_i}, \quad (9)$$

where  $\Phi_i \in (0, 1)$  is the proportion of the node's queue resources allocated to  $f_i$ . Besides, unit resource allocation overhead  $o$  varies considerably across different domains. Typically, satellite resources, such as computing and storage, are relatively scarce and valuable. Additionally, there are significant differences in configuration overhead between terrestrial end domains and forwarding domains. Considering that the end domains adopt two-queue CQF mechanism and the forwarding domains adopt four-queue DIP mechanism, the total resource allocation overhead of the DetSTIN in a time slice can be described as

$$\mathcal{OH} = 2 \sum_{v_x \in D_\alpha} C_{v_x}^{D_\alpha} o^\varphi + 4 \left( \sum_{v_y \in D_\beta} C_{v_y}^{D_\beta} o^\phi + \sum_{v_z \in D_\gamma} C_{v_z}^{D_\gamma} o^\xi \right), \quad (10)$$

where  $v_x$ ,  $v_y$ , and  $v_z$  are nodes in  $D_\alpha$ ,  $D_\beta$ , and  $D_\gamma$ , respectively. In addition,  $o^\varphi$ ,  $o^\phi$ , and  $o^\xi$  are the configuration overheads per unit of resource in the corresponding domains.

2) *Transmission scheduling benefit:* Within each time slice, service flows of different types, characterized by distinct unit gain  $\xi_{f_i}$ , are transmitted and scheduled along pre-planned paths and queues. Delay optimization can effectively improve users' experience, while transmission failure may lead to serious service interruptions or functional degradation. Therefore, we define the transmission scheduling benefit as a weighted combination of the gains brought by delay optimization and the losses caused by transmission failures.

During time slice transitions, it is critical to evaluate whether service flows have been successfully transmitted [51]. We introduce  $\chi_{f_i} \in \{0, 1\}$ , where  $\chi_{f_i} = 1$  indicates successful transmission and  $\chi_{f_i} = 0$  indicates failure. For successful transmission, delay optimization can be evaluated by the delay ratio  $\mathcal{D}_i/D_{f_i}$ , where  $D_{f_i}$  is the delay requirement of  $f_i$ , and  $\mathcal{D}_i$  is the actual transmission delay. Different types of service flows yield varying gains  $\xi_{f_i}$  from delay optimization, with TT flows benefiting the most and BE flows benefiting the least. In contrast, transmission failures, regardless of the type of service flows, may lead to data retransmission and increasing network burden. This impact is particularly significant, especially in highly concurrent or resource-constrained network scenarios. To account for these failures, we introduce a uniform punishment term  $\gamma$ , which represents the average cost of every transmission failures. Combining these factors, the transmission scheduling benefits in a

time slice can be expressed as

$$\mathcal{B} = \sum_{f_i \in \mathcal{F}} \left( \mathbb{I}(\chi_{f_i} = 1) \cdot \xi_{f_i} \cdot \frac{D_{f_i}}{\mathcal{D}_i} - \mathbb{I}(\chi_{f_i} = 0) \cdot \gamma \right), \quad (11)$$

where  $\mathbb{I}(\cdot)$  is the indicator function.  $\mathbb{I}(\cdot) = 1$  denotes successful transmission, while  $\mathbb{I}(\cdot) = 0$  denotes failed transmission.

### III. PROBLEM FORMULATION

To address the heterogeneity of the DetSTIN and achieve seamless and efficient communication, we formulate a multi-objective optimization problem. This problem focuses on optimizing network operation and users' experience by coordinating network resource allocation and on-demand differentiated scheduling, which is formulated as

$$\mathbf{P}_0 : \max_{\mathcal{F}, G_\Gamma} \mathcal{F}(\mathcal{F} | G_\Gamma) \quad (12)$$

$$\text{s.t. } G_\Gamma \in \arg \max_G \mathcal{F}'(G(V, \mathcal{E})). \quad (13)$$

Here,  $\mathcal{F}'(G(V, \mathcal{E}))$  evaluates the performance of the network operation, while  $\mathcal{F}(\mathcal{F} | G_\Gamma)$  quantifies the performance of the users' experience based on the optimized high-performance network  $G_\Gamma$ .

For the network operation, considering cost reduction and efficiency improvement via resource adaptation, it is crucial to achieve flexible resource deployment at non-gateway nodes, obtaining the maximal possible global throughput with minimal overall resource allocation overhead, and ensuring that the nodes have high resource utilization during the transmission of service flows. By introducing three weighting factors  $\Lambda$ ,  $\Gamma$ , and  $\Pi$ , the performance of the network operation can be quantified as

$$\mathbf{P}_{01} : \max \mathcal{F}'(G(V, \mathcal{E})) = \Lambda(1 - \overline{\mathcal{OH}}) + \Gamma \cdot \tau + \Pi \cdot \eta. \quad (14)$$

$$\text{s.t. } \tau \geq \tau^{req}, \quad (14a)$$

$$\eta \geq \eta^{req}. \quad (14b)$$

where  $\Lambda > \Gamma > \Pi$  and  $\Lambda + \Gamma + \Pi = 1$ . Here,  $\overline{\mathcal{OH}}$  represents the normalized resource allocation overhead, which can be calculated by

$$\overline{\mathcal{OH}} = \frac{\mathcal{OH} - \mathcal{OH}_{min}}{\mathcal{OH}_{max} - \mathcal{OH}_{min}}. \quad (15)$$

Besides,  $\tau$  denotes overall network throughput rate via weighted summation, taking into account the maximum transmission capacity of the network under different flow types and the allowed flow number at the entrance, thus

$$\tau = \frac{w_1 A_{TT} + w_2 A_{AVB} + w_3 A_{BE}}{w_1 B_{TT} + w_2 B_{AVB} + w_3 B_{BE}}, \quad (16)$$

where  $A_{flow\_type}$  indicates the maximum number of successfully transmitted flows when all network resources are used to transmit this type of flow, while  $B_{flow\_type}$  indicates the total number of flows allowed to enter at the network entrance, and weights  $w_1$ ,  $w_2$ , and  $w_3$  reflect the priority of resource allocation for different flow types. Here,  $w_1 > w_2 > w_3$  and  $w_1 + w_2 + w_3 = 1$ . Moreover, resource utilization  $\eta$  focuses

more on the effective usage of node resources with the allocated cache resources, which is given by

$$\eta = \frac{\sum_{f_i \in \mathcal{F}} \mathbb{I}(\chi_{f_i} = 1) \cdot |p_{f_i}| \cdot C_{f_i}}{\sum_{v_x \in D_\alpha} 2 \cdot C_{v_x}^{D_\alpha} + 4 \cdot \left( \sum_{v_y \in D_\beta} C_{v_y}^{D_\beta} + \sum_{v_z \in D_\gamma} C_{v_z}^{D_\gamma} \right)}. \quad (17)$$

Here,  $|p_{f_i}|$  reflects the hop count. Note that the throughput rate and resource utilization must satisfy the constraints defined in (14a)–(14b), ensuring they exceed the required thresholds  $\tau^{\text{req}}$  and  $\eta^{\text{req}}$ , respectively.

For the users' experience, we mainly focus on the efficiency of flow transmission. Specifically, the objective is to maximize the scheduling success ratio, while increasing the transmission scheduling benefit via global route planning decisions between time slices and local queue selection decisions within each time slice. This problem can be formally described as

$$\mathbf{P}_{02} : \max_{f_i \in \mathcal{F}} \left( \alpha \cdot \frac{\sum \chi_{f_i}}{|\mathcal{F}|} + \beta \cdot \mathcal{B}(\mathcal{D}_i, \xi_{f_i}) \right), \quad (18)$$

where  $\alpha$  and  $\beta$  are weight parameters satisfying  $\alpha + \beta = 1$  and  $\alpha > \beta$ . Placing excessive emphasis on optimizing the scheduling success ratio may lead to insufficient attention to delay optimization, often resulting in higher overall delay. Conversely, although prioritizing the maximization of transmission scheduling benefits may significantly optimize the delay of individual flows, it can also result in frequent transmission failures, ultimately degrading overall transmission performance. Considering the coupling correlation between these two aspects in problem  $\mathbf{P}_{02}$ , we decouple the problem into two independent subproblems, i.e.,  $\mathbf{P}_1$  and  $\mathbf{P}_2$ .

*Subproblem 1: Global route planning subproblem* is considered in limited network resources to pre-allocate transmission paths. These paths should satisfy delay requirements for each service flow within a time slice as much as possible to ensure a high scheduling success ratio, which can be expressed as

$$\mathbf{P}_1 : \max \sum_{f_i \in \mathcal{F}} \chi_{f_i}. \quad (19)$$

*Subproblem 2: Local queue selection subproblem* seeks to further optimize delay to improve transmission scheduling benefit based on the solutions derived from subproblem 1. Specifically, subproblem 2 focuses on refining the selection of local queues to enhance overall transmission efficiency and performance, while adhering to the pre-allocated resources and constraints established in the global route planning stage. The formulation is given by

$$\mathbf{P}_2 : \max \sum_{f_i \in \mathcal{F}} \frac{D_{f_i}}{\mathcal{D}_i}. \quad (20)$$

Obviously, when each node along the planned global path satisfies the queue resource requirements of the service flow and the E2E delay is within the allowable range, the service flow is considered successfully scheduled. To simplify the problem, we adopt the following convention: if all queues at any node along the transmission path fail to cache the service flow due to insufficient capacity, the scheduling is deemed unsuccessful;

then, actual delay  $\mathcal{D}_i$  of an unsuccessfully scheduled service flow is characterized as times of its upper bound delay  $D_{f_i}$ , thus transforming subproblem  $\mathbf{P}_1$  to subproblem  $\mathbf{P}_2$ . This convention introduces an implicit punitive mechanism, where the impact of transmission failure is reflected as an increase in delay. Consequently, the reduction in the delay ratio effectively captures the loss of transmission failure. As a result,  $\mathbf{P}_2$  not only optimizes transmission scheduling benefits but also unifies the treatment of both successfully and unsuccessfully scheduled flows, thereby fully representing the overall optimization objective of the original coupled problem  $\mathbf{P}_{02}$ .

With the previous analysis, the transmission scheduling problem in the DetSTIN can be transformed into resource adaptation optimization  $\mathbf{P}_{01}$  on the network operation and delay optimization  $\mathbf{P}_2$  on the users' experience, while satisfying the following constraints:

- *Network Resource Constraint:* For node  $v_j$ , the allocation of queue resources must satisfy both lower and upper bounds. The lower bound ensures that flow  $f_i$  passing through the node can be accommodated to prevent large-scale transmission failures due to insufficient resources; the upper bound prevents over-allocation by ensuring that the total queue resources allocated to  $v_j$  do not exceed the total size of all flows within the time slice as not all flows pass through this node. This constraint is expressed as

$$\sum_{f_i \in \mathcal{F}, v_j \in p_{f_i}} C_{f_i} \leq \delta(v_j) C_{v_j} \leq \sum_{f_i \in \mathcal{F}} C_{f_i}. \quad (21)$$

- *Deterministic Transmission Scheduling Constraints:* With the allocated cache resources, the E2E transmission delay of a single flow must be constrained within its allowable delay requirement, i.e.,

$$\mathbb{I}(\chi_{f_i} = 1) \cdot \mathcal{D}_i \leq D_{f_i}, \quad \forall f_i \in \mathcal{F}. \quad (22)$$

For flows that fail to transmit, a delay punishment is imposed to reflect the cost of failure, i.e.,

$$\mathbb{I}(\chi_{f_i} = 0) \cdot \mathcal{D}_i = \partial D_{f_i} (\partial > 1), \quad \forall f_i \in \mathcal{F}, \quad (23)$$

where  $\partial$  is a punitive factor greater than 1, amplifying the delay to represent the impact of unsuccessful scheduling.

- *Network Operation Constraint:* The network operation revenue of the DetSTIN is determined by the balance between the resource allocation overhead and the transmission scheduling benefit. To ensure sustainable operation, it is necessary to avoid a financial deficit, i.e.,  $\mathcal{R} > 0$ .

#### IV. RESOURCE ADAPTATION AND DIFFERENTIATED SCHEDULING ALGORITHMS FOR THE DETSTIN

##### A. Improved Genetic-Based Resource Adaptation Algorithm

To address the resource adaptation problem  $\mathbf{P}_{01}$ , we design an improved genetic-based algorithm, which is based on a fitness indicator, taking the overhead, throughput rate, and resource utilization into consideration. Inspired by the principles of biological evolution, genetic algorithm (GA) simulates the concept of “survival of the fittest”, making it well-suited for global optimization. During the evolution of a population, through

**Algorithm 1:** BUDGET.

**1 Input:** Network topology  $G(V, \mathcal{E})$ , service flow set  $\mathcal{F}$ , iteration round  $M_1$ , population size  $N_1$ , elite ratio  $\sigma$ , and crossover rate  $p_c$ ;

**2 Output:** Optimal intra-domain resource allocation scheme  $s^* = \{res_{v_0}^{M_1}, res_{v_1}^{M_1}, \dots, res_{v_n}^{M_1}\}$ ;

**3 Initialization phase:**

- 4 Extract  $G$  and  $\mathcal{F}$ , and calculate node degrees;
- 5 **for**  $individual \in \{1, \dots, i, \dots, N_1\}$  **do**
- 6   **for**  $node \in \{v_0, v_1, \dots, v_n\}$  **do**
- 7     Randomly allocate resources within the range;
- 8   Form original  $s_i^0 = \{res_{i,v_0}^0, res_{i,v_1}^0, \dots, res_{i,v_n}^0\}$ ;
- 9 Form initial population  $S^0$ ;

**10 Iterative evolution phase:**

- 11 **for**  $generation \in \{1, \dots, j, \dots, M_1\}$  **do**
- 12   **Evaluate fitness:**
- 13   **for**  $individual \in \{1, \dots, i, \dots, N_1\}$  **do**
- 14     Calculate  $fit_i^j = \Lambda(1 - \overline{\mathcal{O}\mathcal{H}}) + \Gamma \cdot \tau + \Pi \cdot \eta$ ;
- 15   **Select Elite:**
- 16   Select  $Elites = Top_\sigma(N_1(\text{SortDesc}(fit)))$  and save to the next generation of the population;
- 17   **Generate new populations:**
- 18   For non-elite individuals, the probability of being selected is  $p_i^j = fit_i^j / \sum_i fit_i^j$ ;
- 19   ▶ Select parents satisfying  $\sum_{k=1}^{i-1} p_k^j < r \leq \sum_{k=1}^i p_k^j$  using Roulette Wheel, where  $r \in [0, 1]$ ;
- 20   ▶ Choose self-folding or crossover to produce offsprings with  $p_c$ ;
- 21   ▶ Mutate offsprings by node degrees with  $p_m$ ;
- 22   Form evolution
- 23    $S^j = \{s_i^j | s_i^j = \{res_{i,v_0}^j, res_{i,v_1}^j, \dots, res_{i,v_n}^j\}\}$ ;
- 23 **return**  $s^* = arg \max_{s_i \in S^{M_1}} fit_i^{M_1}$ .

selection, crossover, and mutation operations, only individuals adapted to the environment are screened out and retained. Traditional GA typically initializes the population randomly within the solution space, ensuring diversity but lacking problem-specific guidance. For network resource allocation problems, a commonly adopted variation of GA (referred to as GAN) generates the initial population based on node degrees, ensuring that nodes with similar degrees start with similar resource allocation. This adjustment aligns the algorithm more closely with the problem's constraints but may limit the diversity of the initial population. Besides, while the introduction of the elitism strategy (referred to as GANE) enhances convergence by retaining the best individuals for the next generation, it also reduces diversity and exacerbates the risk of premature convergence as the search ability diminishes in later stages.

In response to the limitations of these approaches, as shown in Fig. 4, the designed algorithm, named Buffer Utilization baseD on Genetic algorithm for Elastic Transmission (BUDGET), introduces several key enhancements. Unlike GAN and

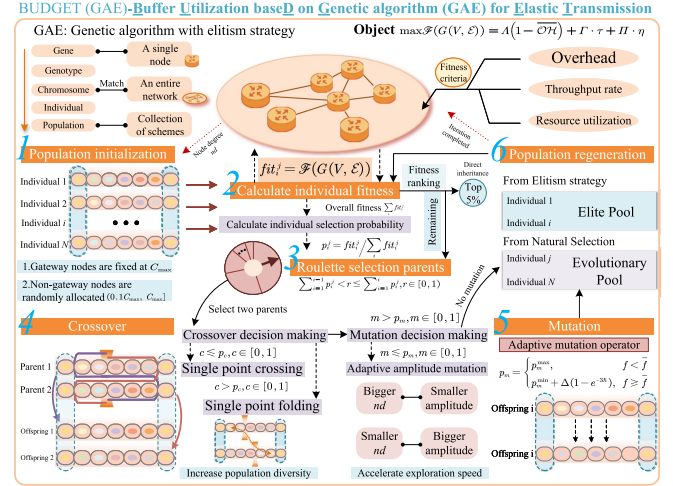


Fig. 4. Improved genetic-based resource adaptation algorithm.

GANE, BUDGET eliminates node degree constraints during initialization by randomly generating an initial population within a reasonable range. During the crossover process, the BUDGET introduces self-folding operation for individuals that do not undergo crossover, further enriching population diversity. In the mutation stage, the BUDGET applies adaptive mutation amplitudes based on node degrees, ensuring that nodes with higher degrees, which typically require more resources due to their central roles in the network, are therefore assigned a higher amount of resources. Conversely, nodes with lower degrees, having less demand for resources, are adjusted toward fewer resources. Additionally, the adaptive mutation operator is correlated with fitness, assigning low-fitness individuals with poor performance a larger mutation probability to encourage exploration. Combined with an elitism strategy, these enhancements increase population diversity, improve targeted exploration, and reduce the number of required evolution generations. In the following, we elaborate the operation process of the BUDGET in detail, which is illustrated in Algorithm 1.

*Population Initialization:* The chromosome encoding in the BUDGET adopts natural number encoding, associating point positions with network node indexes. For each point on every chromosome, a random number is generated within the range  $(0.1 C_{\max}, C_{\max}]$ , representing the amount of node resources, thus forming the initial population. Here,  $C_{\max} = \sum_{f_i \in \mathcal{F}} C_{f_i}$ , and the gateway nodes are fixed at  $C_{\max}$ .

*Select:* The selection process employs a probability-based roulette wheel algorithm, where individuals with higher fitness have a greater chance of passing their genes to the next generation. Fitness directly reflects network performance, lower resource allocation overhead may lead to a higher fitness while maintaining a certain level of throughput rate and resource utilization. Therefore, the fitness function aligns directly with (14), i.e.,

$$fit \triangleq \mathcal{F}'(G(V, \mathcal{E})) \quad (24)$$

$$\text{s.t. (14), (15), (16), and (17).} \quad (24a)$$

In the selection process, we first employ an elitism strategy by directly copying the top 5% of individuals with the highest fitness into the offspring population, and then proceed to select the parents. This strategy aims to ensure that the genetic information of the optimal individuals is preserved, thereby enhancing the stability and convergence speed of the algorithm.

*Self-folding/Crossover:* Once two parents are selected, a random non-gateway node is chosen as the operation point. With a probability of  $p_c$ , a single-point crossover is performed; otherwise, with a probability of  $1 - p_c$ , a single-point self-folding operation is applied. In the case of crossover, the genes of offspring 1 are inherited from parent 1 before the crossover point and from parent 2 after the crossover point, while offspring 2 inherits genes oppositely. For self-folding, the genes of each offspring are mirrored around the selected point, creating one self-reflected offspring.

*Mutation:* For the generated offspring population, which includes both the preserved elite individuals and those produced through the crossover or self-folding of parent individuals, gene mutation is performed with adaptive probability  $p_m$ . The adaptive mutation adjusts the mutation rate dynamically based on the individual and average fitness  $\bar{fit}$  of the population. For individuals with lower fitness, a higher probability of significant mutation is assigned, aiming to discover new potential solutions. The specific form of the mutation operator is

$$p_m = \begin{cases} p_m^{\max}, & fit < \bar{fit}, \\ p_m^{\min} + \Delta(1 - e^{-3\hbar}), & fit \geq \bar{fit}, \end{cases} \quad (25)$$

where  $\Delta = p_m^{\max} - p_m^{\min}$  denotes the difference between the maximal mutation probability and the minimal one, and  $\hbar = (\bar{fit}_{\max} - \bar{fit})/(\bar{fit}_{\max} - \bar{fit}_{\min})$ . Meanwhile, the magnitudes of variation are negatively correlated with node degrees. The larger the node degree, the less resources are reduced or more resources are added per variation. Through this adaptive mutation that differentially considers node degrees, the designed algorithm can quickly converge.

This resource adaptation algorithm achieves a good balance between exploration and exploitation. The adaptive mutation plays a crucial role in exploring new solutions, while the elitism strategy emphasizes the utilization of existing optimal solutions.

## B. Deep RL-Based Deterministic Transmission Scheduling Algorithm

To effectively solve the E2E transmission scheduling problem of mixed service flows within a time slice, we introduce deep RL based on two main considerations:

*First*, flow scheduling problems typically involve large-scale state spaces, multi-objective optimization, and dynamically changing environments. Deep RL, with its ability to handle complex state representations and learn optimal policies through trial-and-error in dynamic settings, is well-suited to address these problems [52]. Additionally, flow scheduling typically pursues long-term or overall performance metrics (such as average delay and overall benefit), and deep RL is naturally suited for optimizing long-term cumulative rewards. *Second*, traditional flow scheduling algorithms rely on preset rules or

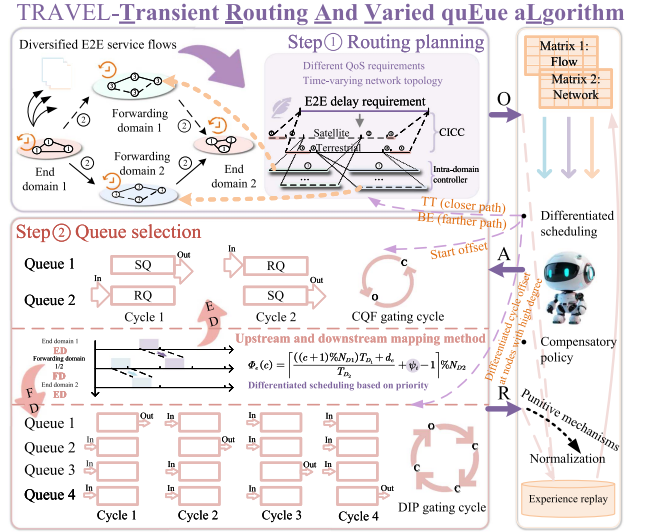


Fig. 5. Deep RL-based deterministic transmission scheduling algorithm.

heuristic methods. However, preset rules are static and designed for specific and simplified scenarios, making it difficult for them to cope with sudden changes in the network environment, such as traffic surges. Meanwhile, heuristic methods, which are based on empirical rules, lack precision when dealing with the fine-grained and dynamic changes in complex networks, and they are unable to adapt to the changing traffic patterns and QoS requirements. In contrast, deep RL has the capability of adaptive decision-making. It learns optimal strategies through continuous interaction with the network environment, enabling the scheduling system to adapt to network changes and autonomously learn optimal decisions from raw inputs without human intervention.

Given these advantages, we formulate the problem as a Markov decision process, which provides the mathematical framework for modeling sequential decision-making problems. With the aim of maximizing transmission scheduling benefit, we then propose the TRAVEL algorithm, which implements a specific deep RL architecture known as Dueling Double Deep Q-Network (D3QN). This advanced variant of deep RL offers improved learning stability and performance by separating value and advantage estimations while reducing overestimation bias, making it particularly suitable for the considered complex scheduling task.

*State Extraction:* As shown in Fig. 5, the agent constructs two state matrices based on environmental inputs to provide the foundation for subsequent scheduling decisions. The first state matrix  $O_t^{req}$  describes the transmission requirements of the service flows, including the source address, destination address, flow size, and transmission delay requirements, which has been defined in (1). The second state matrix records the queue capacity of each node across the domains, which can be denoted by

$$O_t^{cap} = \begin{bmatrix} \mathbb{C}_{v_i,0}^{D_\alpha}(t) & \dots & \mathbb{C}_{v_k,0}^{D_\alpha}(t) & \dots & \mathbb{C}_{v_j,0}^{D_\alpha}(t) \\ \mathbb{C}_{v_i,1}^{D_\alpha}(t) & \dots & \mathbb{C}_{v_k,1}^{D_\alpha}(t) & \dots & \mathbb{C}_{v_j,1}^{D_\alpha}(t) \\ 0 & \dots & \dots & \dots & 0 \\ 0 & \dots & \mathbb{C}_{v_k,3}^{D_\alpha}(t) & \dots & 0 \end{bmatrix}, \quad (26)$$

**Algorithm 2:** TRAVEL.

---

**1 Input:** Network topology  $G(V, \mathcal{E})$ , service flow set  $\mathcal{F}$ , intra-domain resource allocation scheme  $s^*$ , non-aggregation node set  $N_{ld}$ , aggregation node set  $N_{hd}$ , iteration round  $M_2$ , experience replay buffer size  $N_2$ , and exploration rates  $\varepsilon_{ini}$  and  $\varepsilon_{fin}$ , parameter update frequency  $U$ ;

**2 Output:** Global transmission scheduling scheme  $S = \{PATH, QUEUE\}$ ;

**3 Initialize** online and target  $Q$  network parameters  $\theta$  and  $\theta'$ ,  $\theta \rightarrow \theta'$ ,  $\varepsilon_{ini} \rightarrow \varepsilon$ ,  $S = \{\}$ ;

**4 for**  $episode = 1$  to  $M_2$  **do**

**5 Initialize** environment:  $O = O_1$ ;

**6 for**  $flow f_i \in \{f_0, f_1, \dots, f_{|\mathcal{F}|}\}$  **do**

**7 Extract** flow features;

**8 Obtain** all feasible paths with existing cache resources;

**9**  $a_t \leftarrow Q(o_t, a_t, \theta)$  via  $\epsilon$ -greedy policy;

**10 Make** route planning decision  $p_{f_i}$ ;

**11**  $p_{f_i} \rightarrow PATH$ ;

**12 Generate** global route decisions  $PATH$ ;

**13 for**  $node v_k \in \{v_0, v_1, \dots, v_n\}$  **do**

**14 if**  $node v_k$  in  $N_{ld}$  **then**

**15**  $\psi_i = 1$ , relative offset is 0;

**16 if**  $node v_k$  in  $N_{hd}$  **then**

**17 for**  $flow f_j \in \{f_0, f_1, \dots, f_{|\mathcal{F}|}\}$  **do**

**18 if**  $f_j$  is of TT type **then**

**19**  $\psi_i = 1$ , relative offset is 0;

**else**

**21 obtain** relative offset via  $a_t$ ;

**22 Convert** relative offset to the actual queue  $q_{f_j} \leftarrow q_{f_j}^{v_k}$ , and carry out compensatory scheduling;

**23 Collect** queue selection decision  $q_{f_j} \rightarrow QUEUE$ , and observe reward  $r_t$  and new state  $o_{t+1}$ ;

**24 Store** tuple  $\{o_t, a_t, r_t, o_{t+1}\}$  into *Buffer*;

**25 Sample** a random minibatch of tuples from *Buffer*;

**26 Update**  $\theta \rightarrow \theta'$  every  $U$  steps.

**27 return**  $S = \{PATH, QUEUE\}$ .

---

where  $\mathbb{C}_{v_i,s}^{D_\alpha}$  and  $\mathbb{C}_{v_j,s}^{D_\alpha}$  represent the remaining capacities of the  $s$ -th queue of node  $v_i$  and  $v_j$  in domain  $D_\alpha$ , respectively, and  $\mathbb{C}_{v_k,\Delta,s}^{D_\Delta}$  denotes the remaining capacity of the  $s$ -th queue of node  $v_k$  in  $D_\Delta$ ,  $\forall \Delta \in \{\beta, \gamma\}$ . Thus, the network state can be defined as  $O = \{O_t^{req}, O_t^{cap}\}$ .

*Decision Execution:* Based on these two state matrices, the agent adopts a differentiated scheduling algorithm that acts in two stages, which can be characterized by a two-dimensional tuple  $(path, queue)$ , i.e.,

$$A = \{a_t \mid a_t = (p_{f_i}, q_{v_j})\}, \\ q_{v_j} \in [\min\{1, \delta(v_j) - 2\}, \max\{1, \delta(v_j) - 2\}] \}. \quad (27)$$

$$\text{s.t. (2).} \quad (28)$$

The first stage involves a global decision, where the agent selects an appropriate E2E transmission path according to the QoS requirements of the service flows. This path selection is a two-step process: First, an appropriate transmission media (i.e., satellite or terrestrial network) is selected. Then, based on the chosen media, the specific E2E route is determined according to the feasible segment routing information feedback from each domain to ensure the path satisfies the delay and reliability requirements of the service flows. Second, the agent proceeds to the second stage of local scheduling decisions. In this stage, the agent selects an appropriate sending queue at the source node to determine the sending time of the service flow. Additionally, if the flow is AVB or BE type, the agent selects a maximum waiting delay to determine the queue offset. That is, when  $\delta(v_j) = 2$ , which means at the source node in the end domain, the agent chooses from  $[0, 1]$  to decide whether the flow enters the receiving queue and will be forwarded in the next cycle, or the flow waits one cycle to enter and will be forwarded two cycles later. When  $\delta(v_j) = 4$ , which means at the nodes with high node degree in the forwarding domain, the agent chooses from  $[1, 2]$  to decide the offset of AVB or BE flows.

If the local scheduling decision in the second stage fails to satisfy the delay requirements or if the cache capacity of the node is insufficient, a compensatory policy is triggered to try to reschedule. This policy automatically effectuates to ensure the service flow is transmitted within the global delay requirement, without requiring further agent intervention.

*Reward Acquisition:* Upon completing the scheduling decision, the agent receives a corresponding reward. This reward is directly linked to the delay optimization of the service flows, with higher rewards obtained for unit delay optimization of TT flows compared to BE flows. In case of transmission failures, uniform negative reward  $P$  is feedback without discrimination, i.e.,

$$r_t = \begin{cases} \xi_{f_i} \left( \frac{D_{f_i}}{\mathcal{D}_i} \right), & \chi_{f_i} = 1, \\ P, & \chi_{f_i} = 0. \end{cases} \quad (29)$$

As a result, the agent prioritizes the optimization of TT and AVB flows, placing delay optimization of BE flows the lower priority. A well-designed reward function helps to accelerate the agent's learning process, enabling it to converge efficiently toward optimal scheduling strategies. Finally, the agent stores the current state, decision, and reward information into an experience replay buffer before transitioning into the next state to continue the decision-making process. Through iterative optimization, the agent gradually improves its scheduling performance for different service flows, enhancing overall transmission performance of the DetSTIN.

The algorithm optimizes transmission scheduling in the DetSTIN by considering flow requirements and network resources simultaneously. The state transition and training processes are detailed in Algorithm 2.

TABLE I  
NETWORK CONFIGURATION

Parameter	Value	Parameter	Value
$Num_{GEO}, Num_{LEO}$	3, 7	$Num_{router}^{D_{sat}}, Num_{router}^{D_{ter}}$	2, 1
$\mathcal{L}_s$	300km	$\mathcal{L}_t$	200km
$V_s(\text{laser})$	$3 \times 10^8 \text{ m/s}$	$V_t(\text{optical fiber})$	$2.05 \times 10^8 \text{ m/s}$
$B_s, B_f$	1Gbps	$B_d$	2Gbps
$T_{v_j}^{D_s}$	30μs	$T_{v_j}^{D_s}, T_{v_j}^{D_{ter}}$	15μs
$C_f^{TT}, C_f^{AVB}, C_f^{BE}$	{16000, 26000, 4000}bit	$D_f^{TT}, D_f^{AVB}, D_f^{BE}$	{5.14, 6.28, 7.32}ms

TABLE II  
FLOW PROPORTION

Flow Proportion	Actual Flow Number (TT AVB BE)	Actual Traffic Ratio (TT AVB BE)
1	30 50 20	0.30: 0.50: 0.20
2	26 50 36	0.23: 0.45: 0.32
3	20 50 60	0.15: 0.38: 0.46
4	16 50 76	0.11: 0.35: 0.54
5	10 50 100	0.06: 0.31: 0.63

## V. SIMULATION RESULTS

### A. Experimental Setup

We conduct extensive simulations to evaluate the performance of the proposed resource adaptation algorithm BUDGET and differentiated scheduling algorithm TRAVEL. Below we introduce the key components of the simulation. The main simulation parameters are listed in Table I.

First, we consider a typical STIN scenario, where 7 nodes in the satellite forwarding domain and 7 nodes in the terrestrial forwarding domain are deployed. Satellites locate 1,000 km above the terrestrial, and a set of mixed flows generated at two source nodes is forwarded to the same destination node via forwarding domains. The distance between adjacent nodes is set to  $\mathcal{L}_s$  for LEOs and  $\mathcal{L}_t$  for terrestrial nodes. Laser technologies are adopted to satellite-terrestrial and inter-satellite communication with a propagation speed of  $3 \times 10^8 \text{ m/s}$ , while terrestrial nodes utilize fiber optic communication with a propagation speed of  $2.05 \times 10^8 \text{ m/s}$ . The bandwidths of source domain and forwarding domains are both configured to 1 Gbps, while the bandwidth of destination domain is set to 2 Gbps [53]. We intercept and construct three types of service flows from the *iot\_data dataset* provided by Alibaba Cloud Tianchi, in which the size and delay requirement are listed in Table I. The initial configuration of the mixed flows consists of 100 flows, with TT, AVB, and BE flows in a ratio of 3:5:2. Furthermore, we assume the total demand for service flow transmission within a time slot (i.e., total size of service flows) remains constant, while the proportion of service flows changes as shown in Table II. As the flow proportion changes from 1 to 5, the proportion of BE flow increases. Second, for resource adaptation, the weighting factors of fitness  $\Lambda$ ,  $\Gamma$ , and  $\Pi$  are set to 0.5, 0.3, and 0.2, respectively. Besides, the weights  $w_1$ ,  $w_2$ , and  $w_3$  are set to 0.6, 0.3, and 0.1, respectively, to expand the impact of transmission failure of TT flows on throughput rate. Third, for differentiated scheduling, to accelerate the learning speed, the TRAVEL adopts two identical

dual neural networks, with their parameters synchronized every 4 steps. The neural network includes a convolutional neural network and two fully-connected layers. Specifically, we set the learning rate of Adam to be  $10^{-4}$ , and set discount factor and minibatch size to be 0.98 and 64, respectively. In addition, uniform negative reward  $P$  is set to -10.

### B. Convergence and Effectiveness Verification

To evaluate the convergence performance and effectiveness of the two proposed algorithms, we conduct comparative experiments under varying flow proportions separately.

1) *Resource adaptation*: To evaluate the performance of the proposed resource adaptation algorithm, we compare BUDGET with three benchmark algorithms: GA, GAN, and GANE.

As shown in Figs. 6 and 7, the proposed BUDGET algorithm consistently demonstrates the fastest convergence under varying flow proportions, while achieving the highest fitness with minimal resource allocation. When comparing algorithms that consider node degrees during initialization (i.e., GAN and GANE) with those that use random initialization (i.e., GA and BUDGET), the latter achieves higher fitness and allocates fewer resources. This is because initializing based on node degrees reduces population diversity, which slows down the evolutionary process and even cause stagnation. In contrast, random initialization provides greater diversity, enabling faster and more effective optimization. Additionally, algorithms incorporating an elitism strategy (i.e., GANE and BUDGET) exhibit greater stability. This is because the elitism strategy ensures that the best solutions are retained across generations, preventing the loss of optimal individuals and ensuring that fitness does not decrease during the evolutionary process.

As shown in Fig. 8, we evaluate the performance of network operation when cache resources are configured via resource adaptation algorithms under the condition that the total size of flows remains the same but the flow proportion varies. The results indicate that the proposed BUDGET can minimize resource allocation overhead due to weighting factor  $\Lambda$  is set to the largest. In addition, with fewer resource allocation, the BUDGET still achieves good performance in throughput rate and resource utilization. However, the throughput rate and resource utilization of the BUDGET is slightly lower than other algorithms when flow proportion is 4 or 5. The reason is that the cache resource allocation scheme designed specifically for scenarios with a large proportion of BE flows usually tends to distribute resources to multiple hops to satisfy the multi-hop routing requirements of BE flows. On the one hand, resource dispersion exerts a negative influence on the transmission of TT flows. Typically, TT flows follow routes with a relatively fewer hops. When resources are distributed to multiple hops, TT flows may encounter scheduling failures due to the limited cache capacities of nodes, thereby leading to a low throughput rate. On the other hand, resource dispersion also poses a challenge to the full utilization of node cache resources. Nevertheless, the BUDGET still exhibits the high fitness due to its best comprehensive performance regarding these three metrics.

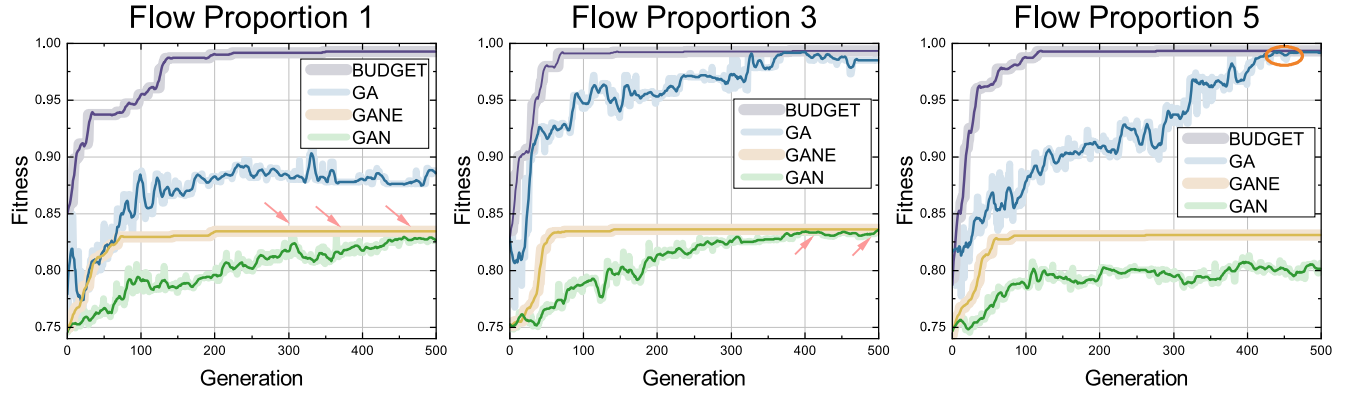


Fig. 6. Fitness over generations under different flow proportions.

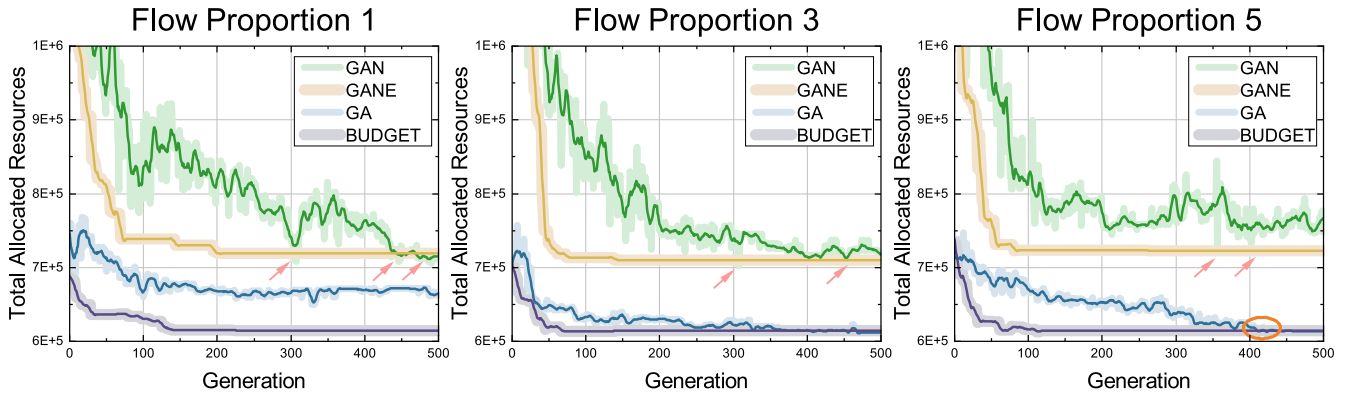


Fig. 7. Total allocated resources over generations under different flow proportions.

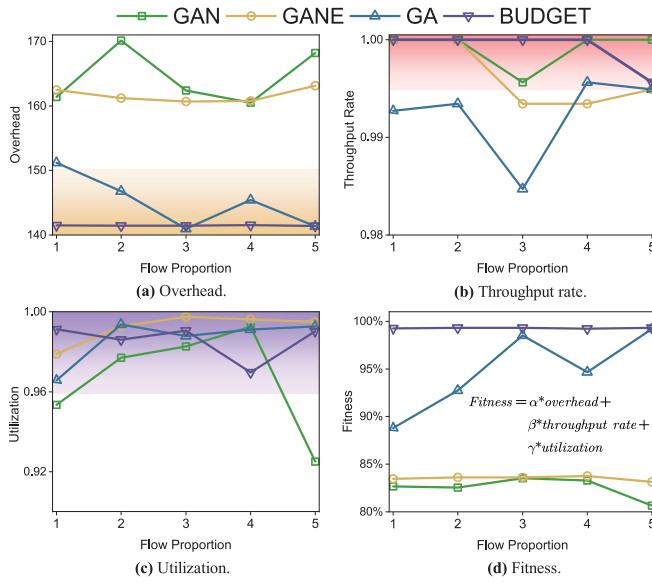
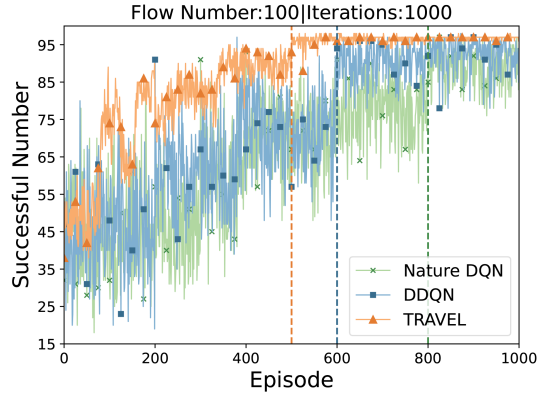


Fig. 8. Evaluation of resource adaptation performance across various metrics.

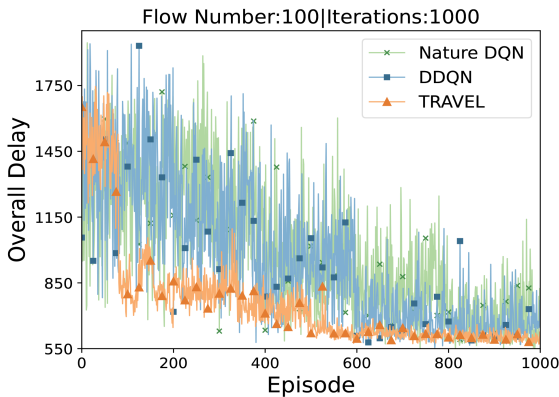
**2) Transmission scheduling:** To evaluate the convergence performance of the proposed TRAVEL, we conduct comparative experiments by replacing the deep RL module from D3QN

with the double deep Q-network (DDQN) and the nature deep Q-network (Nature DQN), our focus is placed on the scheduling success ratio depicted in Fig. 9(a) and the overall transmission delay depicted in Fig. 9(b). As observed, D3QN-based TRAVEL achieves convergence 100 rounds ahead of DDQN and 300 rounds ahead of Nature DQN with high stability. The reason is that D3QN can better estimate the Q-value by considering both the state value function and the advantage function without increasing model complexity, thereby improving the algorithm performance.

To evaluate the effectiveness of the proposed TRAVEL, we then compare it with four benchmark transmission scheduling algorithms under flow proportion 1, namely *Naive* algorithm that flows forward immediately after generate following the shortest path priority principle, multi-path transmission scheduling *MultiDTS*, multi-path transmission with differentiated queue scheduling *MultiDDTS*, and deterministic transmission scheduling *CCDDTS* combining CQF and DIP [53]. In these algorithms, all feasible paths are obtained from CICC, thereby avoiding redundant exploration at the beginning of transmission scheduling. Differentiated scheduling assigns priority labels to different service flows and achieves time isolation through differentiated queue entry, while non-differentiated scheduling *MultiDTS* and *CCDDTS* treats all equally and follows first-in-first-out principle. As shown in Fig. 10(a), when the proportion of TT



(a) Scheduling success ratio.

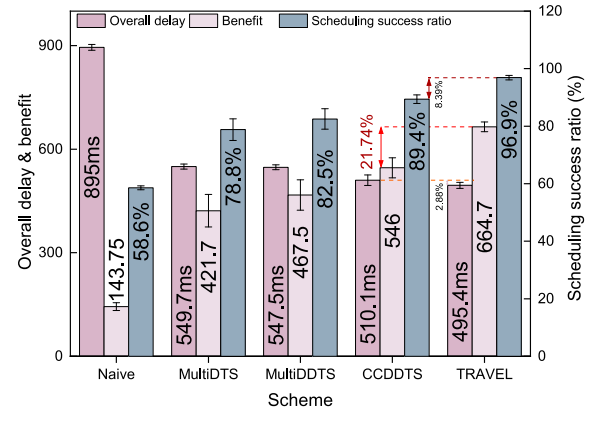


(b) Overall delay.

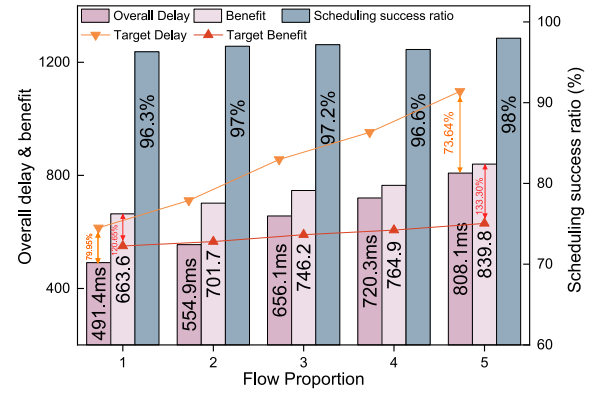
Fig. 9. Convergence performance of different deep RL-based algorithms.

flows is high, the TRAVEL achieves a high scheduling success ratio and low overall delay, thus obtaining the highest transmission scheduling benefit while exhibiting the least fluctuation. Compared to the best benchmark *CCDDTS*, the TRAVEL achieves a 8.39% increase in scheduling success ratio and a 2.88% reduction in overall transmission delay, resulting in a 21.74% increase in transmission scheduling benefit. Besides, with pairwise comparison, it is evident that deep RL online routing outperforms multi-path algorithms, and differentiated scheduling outperforms unified scheduling. Moreover, performance improvements resulting from effective large-scale path selection surpass those from small-scale queue selection. Specifically, for *MultiDTS*, the benefit gain brought by optimizing the path selection (namely *MultiDTS* to *CCDDTS*) is 2.7 times than that of optimizing the queue selection (namely *MultiDTS* to *MultiDDTS*).

The above experiment verifies the effectiveness and reliability of the TRAVEL in scenarios such as the industrial IoT where TT flows account for a large proportion. However, in practical applications, given that the majority of service flows in the network is BE, to validate the general applicability of the TRAVEL, we conduct comparative experiments with different proportions of BE flows under the same network resource settings (namely the total size of the flows and the allocation of network resources are constant). Fig. 10(b) indicates that as the proportion of BE



(a) Different algorithms.



(b) Different flow proportions.

Fig. 10. Performance under different algorithms/flow proportions.

flows increases, there is a general upward trend in the scheduling success ratio, the gains between the overall delay and target delay increases, and the benefits also largely exceed the expected targets, as BE flows have more flexibility and delay tolerance. Specifically, the overall delay decreases from 79.95% of the target delay to 73.64%, and the benefit increases from 120.65% of the target benefit to 133.30% .

### C. Verification for BUDGET and TRAVEL Collaboration

The effectiveness and reliability of resource adaptation algorithm and transmission scheduling algorithm have been individually verified. However, in real-world application scenarios, resource allocation and service flow transmission scheduling should be considered simultaneously, for that the mismatches in resource allocation may lead to significant increases in transmission scheduling delay, thereby being conducive to the deterministic guarantee of service flows. Furthermore, over-allocating resources may result in increased resource allocation overhead, while under-allocation may exacerbate delay in transmission scheduling or even lead to scheduling failures. Given these considerations, we conduct experimental verification on the joint optimization performance of these two algorithms under flow proportion 1, aiming to ensure their synergistic operation in practical applications and mitigate potential performance degradation issues. As shown in

TABLE III  
COLLABORATIVE VERIFICATION RESULTS

Flow number	Transmission scheduling algorithm	Resource adaptation algorithm & scheduling success ratio				Resource adaptation algorithm & overall delay				Resource adaptation algorithm & network operation revenue					
		GAN	GANE	GA	BUDGET	GAN	GANE	GA	BUDGET	GAN	GANE	GA	BUDGET		
100	MultiDTS	81.62	83.84	68.19	60.46	-	548.65	548.29	555.28	-	277.59	301.74	115.64	35.29	
	MultiDDTS	83.17	83.98	69.49	60.75	-	548.38	547.45	551.54	-	299.96	300.17	128.44	40.72	
	CCDDTS	94.59	91.61	93.52	93.68	-	503.96	515.40	501.81	500.29	-	466.35	413.32	468.57	485.84
	TRAVEL	98.00	98.00	98.00	98.00	-	479.22	489.46	465.95	458.71	-	538.07	517.36	562.21	584.82
300	MultiDTS	78.31	80.74	66.74	64.87	-	1622.50	1614.43	1637.21	1640.33	-	676.44	735.96	311.80	271.60
	MultiDDTS	81.38	80.52	67.60	64.79	-	1617.44	1614.00	1636.67	1635.95	-	788.06	733.07	345.82	267.68
	CCDDTS	88.35	87.96	89.27	90.35	-	1494.24	1516.94	1469.17	1448.39	-	1133.40	1082.62	1269.58	1339.59
	TRAVEL	99.33	99.33	99.33	99.33	-	1418.61	1455.49	1341.25	1317.11	-	1627.52	1566.84	1792.13	1835.50
500	MultiDTS	80.48	79.34	71.71	63.11	-	2687.94	2687.95	2680.51	2729.43	-	1259.34	1217.91	878.65	402.83
	MultiDDTS	83.82	83.16	72.53	61.95	-	2679.02	2678.99	2681.06	2720.89	-	1473.39	1461.11	942.01	326.94
	CCDDTS	88.52	87.24	88.78	89.74	-	2450.53	2488.11	2418.30	2388.99	-	1986.58	1868.97	2154.27	2273.77
	TRAVEL	99.60	99.60	99.60	99.60	-	2373.48	2405.97	2204.93	2168.03	-	2721.47	2691.31	3087.10	3164.26
700	MultiDTS	72.15	81.17	68.40	63.09	-	3783.95	3750.81	3791.36	3808.73	-	1211.00	1854.67	950.01	571.32
	MultiDDTS	72.82	83.27	69.49	63.90	-	3779.94	3742.15	3789.34	3799.05	-	1268.86	2043.47	1045.60	648.04
	CCDDTS	87.60	85.80	88.75	88.74	-	3417.06	3480.23	3339.28	3355.77	-	2808.77	2459.18	3054.15	3061.30
	TRAVEL	99.71	99.71	99.71	99.71	-	3170.73	3355.93	3064.48	3032.55	-	4160.93	3782.82	4342.04	4443.47

Table III, the results indicate that the collaboration between the two algorithms still adheres to the performance demonstrated by a single algorithm under different numbers of service flows.

In scenarios with different numbers of mixed service flows, when using the same resource adaptation algorithm (i.e., corresponding to the same node resource allocation and its overhead), the TRAVEL algorithm achieves the highest scheduling success ratio, the lowest overall transmission delay, and the highest transmission scheduling benefit compared to other transmission scheduling algorithms (i.e., the highlighted gray area). This indicates that the TRAVEL algorithm can efficiently complete transmission scheduling and optimize system performance when resource allocation is relatively fixed.

Meanwhile, when different resource adaptation algorithms are jointly optimized with the same transmission scheduling algorithm, there is a significant difference in performance. Although the proposed BUDGET algorithm allocates relatively fewer resources as verified in the previous experiment, it does not affect the transmission scheduling of service flows. On the contrary, the combination scheme of BUDGET and TRAVEL achieves the best transmission scheduling and network operation performance (i.e., blue values), which demonstrates the advantages of the organic combination of the proposed resource adaptation algorithm and differentiated transmission scheduling algorithm.

In addition, under the same transmission scheduling algorithm, the BUDGET algorithm has achieved a certain degree of optimization in terms of scheduling success ratio and overall transmission delay. This optimization effect is attributed to the fact that the BUDGET algorithm is specifically designed to satisfy transmission scheduling requirements, ensuring effective collaboration between algorithms and thus improving overall performance.

However, under GA and BUDGET resource adaptation algorithms that allocate relatively fewer resources, MultiDTS and MultiDDTS algorithms are difficult to adapt to intelligent resource allocation due to their lack of flexibility. This results in a significant decrease in their transmission scheduling

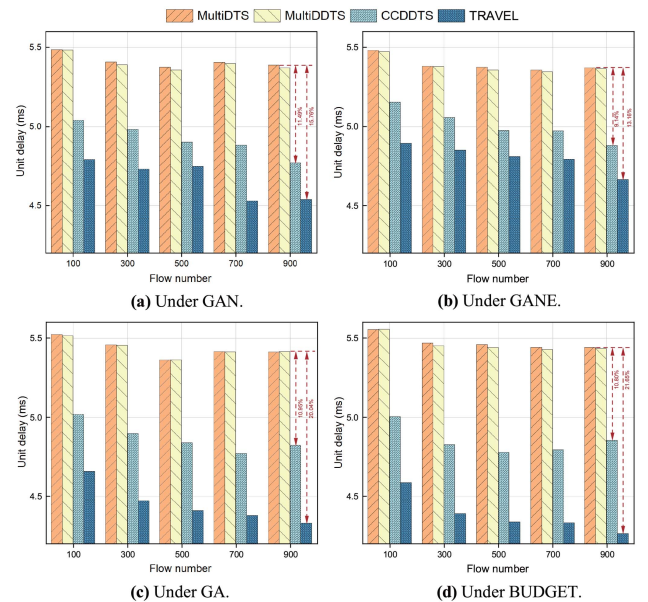


Fig. 11. Unit delay with different flow numbers.

performance, forming abnormal areas in the table (marked by blue dashed boxes). This indicates that in resource-constrained scenarios, the flexibility and adaptability of algorithms are crucial for transmission scheduling performance.

#### D. Scalability Verification

To further verify the effectiveness and scalability of the proposed algorithms, we conduct a comparative analysis of the unit delay with different flow number as shown in Fig. 11 and unit network operation revenue as shown in Fig. 12 for each joint scheme under the condition of flow proportion 1.

As shown in Fig. 11, compared with other transmission scheduling algorithms, TRAVEL demonstrates a significant advantage in reducing unit transmission delay under the same resource adaptation algorithm. More importantly, as the number of flows increases, while other algorithms exhibit varying

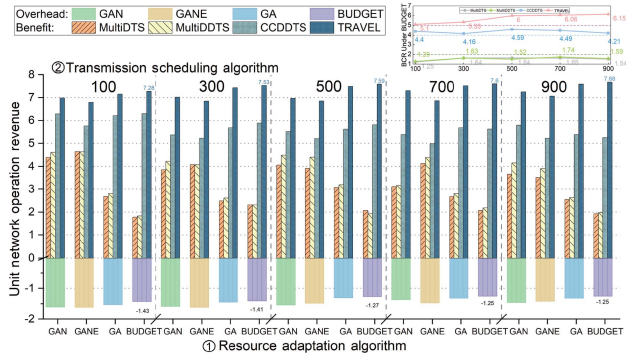


Fig. 12. Unit revenue with different flow numbers.

degrees of fluctuation, the TRAVEL shows a monotonic decreasing trend. This validates TRAVEL's stability and efficiency in handling large-scale service flows. Additionally, the proposed BUDGET algorithm contributes to the optimization of unit transmission delay, further confirming the positive impact of resource adaptation algorithms on overall network performance.

The unit network operation revenue is composed of unit network resource allocation overhead and unit transmission scheduling benefit, represented by positive and negative values, respectively. As shown in Fig. 12, for the resource adaptation algorithms, the proposed BUDGET achieves the lowest resource allocation overhead, and as the number of service flows increases, the unit resource allocation overhead gradually decreases. This indicates that BUDGET has significant advantages in efficient resource utilization, particularly in scenarios with intensive service flows, where their resource optimization capabilities become more prominent. For the transmission scheduling algorithms, the proposed TRAVEL consistently achieves the highest transmission scheduling benefit. Besides, as the number of service flows continues to increase, the unit transmission scheduling benefit increases slightly. This phenomenon validates the effectiveness of TRAVEL in large-scale flow scheduling. Additionally, the upper right corner of Fig. 12 shows the benefit-cost ratio (BCR) for different transmission scheduling algorithms under the BUDGET. It can be seen that the TRAVEL consistently maintains the highest BCR, and unlike other transmission scheduling algorithms that fluctuate, TRAVEL achieves a stable rise.

In conclusion, the proposed BUDGET and TRAVEL algorithms exhibit significant collaborative optimization effects in resource adaptation and transmission scheduling. Especially with the growth of service flows, the two algorithms effectively increase network operation revenue across different dimensions, while also revealing the trade-off between resource allocation overhead and benefit. This provides valuable insights for efficient network resource management.

## VI. CONCLUSION

In this paper, we have investigated a deterministic transmission scheduling problem in the STIN. We have proposed the DetSTIN architecture that combines a flexible resource adaptation algorithm and a differentiated scheduling algorithm,

aiming at providing E2E deterministic transmission guarantees for service flows with diverse QoS requirements in heterogeneous networks. For resource adaptation, we have implemented an improved genetic-based BUDGET algorithm, which dynamically allocates cache resources across intra-domain nodes to ensure optimal cache provisioning for service flows. For differentiated scheduling, we have proposed a deep RL-based TRAVEL algorithm, which operates based on the decisions made by BUDGET, enabling large-scale path optimization and fine-grained queue management at the node level, thereby constructing an E2E dedicated transmission channel for service flows. The combination of these two algorithms facilitates transparent transmission, allowing network operators to reasonably optimize resource allocation while improving the delivery efficiency of service flows. For the future work, we will study an unified identification scheme to enhance management efficiency in the DetSTIN.

## REFERENCES

- [1] W. Zhang, P. Liao, D. Yang, P. Dong, H. Peng, and H. Zhang, "TRAVEL: Deterministic transmission scheduling for satellite-terrestrial integrated networks," in *Proc. IEEE/CIC Int. Conf. Commun. China*, 2024, pp. 1133–1138.
- [2] S. Chen, Y.-C. Liang, S. Sun, S. Kang, W. Cheng, and M. Peng, "Vision, requirements, and technology trend of 6G: How to tackle the challenges of system coverage, capacity, user data-rate and movement speed," *IEEE Wireless Commun.*, vol. 27, no. 2, pp. 218–228, Apr. 2020.
- [3] Q. Ye, J. Li, K. Qu, W. Zhuang, X. S. Shen, and X. Li, "End-to-end quality of service in 5G networks: Examining the effectiveness of a network slicing framework," *IEEE Veh. Technol. Mag.*, vol. 13, no. 2, pp. 65–74, Jun. 2018.
- [4] J. Liu, Y. Shi, Z. M. Fadlullah, and N. Kato, "Space-air-ground integrated network: A survey," *IEEE Commun. Surveys Tut.*, vol. 20, no. 4, pp. 2714–2741, Fourth Quarter, 2018.
- [5] M. Giordani, M. Polese, M. Mezzavilla, S. Rangan, and M. Zorzi, "Toward 6G networks: Use cases and technologies," *IEEE Commun. Mag.*, vol. 58, no. 3, pp. 55–61, Mar. 2020.
- [6] W. Zhang et al., "VSpatial: Enabling private and verifiable spatial keyword-based positioning in 6G-oriented IoT," *IEEE J. Sel. Areas Commun.*, vol. 42, no. 10, pp. 2954–2969, Oct. 2024.
- [7] Y. Liu, L. Wang, Z. Lu, K. Du, and G. Shou, "A stateless design of satellite-terrestrial integrated core network and its deployment strategy," *IEEE Trans. Netw. Service Manag.*, vol. 21, no. 1, pp. 953–966, Feb. 2024.
- [8] X. Zhu and C. Jiang, "Integrated satellite-terrestrial networks toward 6G: Architectures, applications, and challenges," *IEEE Internet Things J.*, vol. 9, no. 1, pp. 437–461, Jan. 2022.
- [9] C. Lei, W. Feng, P. Wei, Y. Chen, N. Ge, and S. Mao, "Edge information hub: Orchestrating satellites, UAVs, MEC, sensing and communications for 6G closed-loop controls," *IEEE J. Sel. Areas Commun.*, vol. 43, no. 1, pp. 5–20, Jan. 2025.
- [10] J. Tang et al., "Opportunistic content-aware routing in satellite-terrestrial integrated networks," *IEEE Trans. Mobile Comput.*, vol. 23, no. 11, pp. 10460–10474, Nov. 2024.
- [11] B. Xie, H. Cui, I. W.-H. Ho, Y. He, and M. Guizani, "Computation offloading and resource allocation in LEO satellite-terrestrial integrated networks with system state delay," *IEEE Trans. Mobile Comput.*, vol. 24, no. 3, pp. 1372–1385, Mar. 2025.
- [12] T. Li, H. Zhou, H. Luo, and S. Yu, "SERvICE: A software defined framework for integrated space-terrestrial satellite communication," *IEEE Trans. Mobile Comput.*, vol. 17, no. 3, pp. 703–716, Mar. 2018.
- [13] X. Zhang et al., "Cost-effective hybrid computation offloading in satellite-terrestrial integrated networks," *IEEE Internet Things J.*, vol. 11, no. 22, pp. 36786–36800, Nov. 2024.
- [14] Y. Lyu, H. Hu, R. Fan, Z. Liu, J. An, and S. Mao, "Dynamic routing for integrated satellite-terrestrial networks: A constrained multi-agent reinforcement learning approach," *IEEE J. Sel. Areas Commun.*, vol. 42, no. 5, pp. 1204–1218, May 2024.

- [15] S. Yao, J. Guan, Z. Yan, and K. Xu, "SI-STIN: A smart identifier framework for space and terrestrial integrated network," *IEEE Netw.*, vol. 33, no. 1, pp. 8–14, Jan./Feb. 2019.
- [16] M. H. Eiza and A. Raschellà, "A hybrid SDN-based architecture for secure and QoS aware routing in space-air-ground integrated networks (SAGINs)," in *Proc. IEEE Wireless Commun. Netw. Conf.*, 2023, pp. 1–6.
- [17] H. A. Shah, L. Zhao, and I.-M. Kim, "Joint network control and resource allocation for space-terrestrial integrated network through hierachal deep actor-critic reinforcement learning," *IEEE Trans. Veh. Technol.*, vol. 70, no. 5, pp. 4943–4954, May 2021.
- [18] Y. Cheng, W. Zhang, Z. Zhang, C. Zhang, S. Wang, and S. Mao, "Towards federated large language models: Motivations, methods, and future directions," *IEEE Commun. Surveys Tut.*, early access, Nov. 21, 2024, doi: [10.1109/COMST.2024.3503680](https://doi.org/10.1109/COMST.2024.3503680).
- [19] W. Zhang, Y. He, T. Zhang, C. Ying, and J. Kang, "Intelligent resource adaptation for diversified service requirements in industrial IoT," *IEEE Trans. Cogn. Commun. Netw.*, early access, Nov. 19, 2024, doi: [10.1109/TCCN.2024.3502493](https://doi.org/10.1109/TCCN.2024.3502493).
- [20] C.-Q. Dai, S. Li, J. Wu, and Q. Chen, "Distributed user association with grouping in satellite-terrestrial integrated networks," *IEEE Internet Things J.*, vol. 9, no. 12, pp. 10244–10256, Jun. 2022.
- [21] H. Hao, C. Xu, W. Zhang, S. Yang, and G.-M. Muntean, "Joint task offloading, resource allocation, and trajectory design for multi-UAV cooperative edge computing with task priority," *IEEE Trans. Mobile Comput.*, vol. 23, no. 9, pp. 8649–8663, Sep. 2024.
- [22] Y. He, J. Fang, F. R. Yu, and V. C. Leung, "Large language models (LLMs) inference offloading and resource allocation in cloud-edge computing: An active inference approach," *IEEE Trans. Mobile Comput.*, vol. 23, no. 12, pp. 11253–11264, Dec. 2024.
- [23] Y. Wu, H.-N. Dai, H. Wang, Z. Xiong, and S. Guo, "A survey of intelligent network slicing management for Industrial IoT: Integrated approaches for smart transportation, smart energy, and smart factory," *IEEE Commun. Surveys Tut.*, vol. 24, no. 2, pp. 1175–1211, Second Quarter, 2022.
- [24] Z. Xiao et al., "LEO satellite access network (LEO-SAN) toward 6G: Challenges and approaches," *IEEE Wireless Commun.*, vol. 31, no. 2, pp. 89–96, Apr. 2024.
- [25] W. Xiang, K. Yu, F. Han, L. Fang, D. He, and Q.-L. Han, "Advanced manufacturing in Industry 5.0: A survey of key enabling technologies and future trends," *IEEE Trans. Ind. Inform.*, vol. 20, no. 2, pp. 1055–1068, Feb. 2024.
- [26] T. Nie et al., "Hierarchical scheduling mechanism based on relaxed constraints for complex industrial scenes," *IEEE Trans. Netw. Sci. Eng.*, vol. 11, no. 3, pp. 3237–3249, May/Jun. 2024.
- [27] H. Yu, T. Taleb, and J. Zhang, "Deep reinforcement learning-based deterministic routing and scheduling for mixed-criticality flows," *IEEE Trans. Ind. Inform.*, vol. 19, no. 8, pp. 8806–8816, Aug. 2023.
- [28] J. Sasain, D. Franco, A. Atutxa, J. Astorga, and E. Jacob, "Towards the integration and convergence between 5G and TSN technologies and architectures for industrial communications: A survey," *IEEE Commun. Surveys Tut.*, vol. 27, no. 1, pp. 259–321, Feb. 2025.
- [29] B. Varga, J. Farkas, F. Fejes, J. Ansari, I. Moldován, and M. Máté, "Robustness and reliability provided by deterministic packet networks (TSN and DetNet)," *IEEE Trans. Netw. Service Manag.*, vol. 20, no. 3, pp. 2309–2318, Sep. 2023.
- [30] H. Bai, H. Li, J. Que, M. Zhang, and P. H. J. Chong, "DSCCP: A differentiated service-based congestion control protocol for information-centric networking," in *Proc. IEEE Wireless Commun. Netw. Conf.*, 2022, pp. 1641–1646.
- [31] C. Makridis, C. Menelaou, S. Timotheou, and C. G. Panayiotou, "A real-time demand management and route-guidance system for eliminating congestion," *IEEE Intell. Transp. Syst. Mag.*, vol. 16, no. 6, pp. 86–104, Nov./Dec. 2024.
- [32] G. Peng, S. Wang, Y. Huang, R. Huo, T. Huang, and Y. Liu, "Traffic shaping at the edge: Enabling bounded latency for large-scale deterministic networks," in *Proc. IEEE Int. Conf. Commun. Workshops*, 2021, pp. 1–6.
- [33] A. Nasrallah et al., "Ultra-low latency (ULL) networks: The IEEE TSN and IETF DetNet standards and related 5G ULL research," *IEEE Commun. Surveys Tut.*, vol. 21, no. 1, pp. 88–145, First Quarter, 2019.
- [34] Y. Zhang, Q. Xu, L. Xu, C. Chen, and X. Guan, "Efficient flow scheduling for industrial time-sensitive networking: A divisibility theory-based method," *IEEE Trans. Ind. Inform.*, vol. 18, no. 12, pp. 9312–9323, Dec. 2022.
- [35] D. Yang et al., "DetFed: Dynamic resource scheduling for deterministic federated learning over time-sensitive networks," *IEEE Trans. Mobile Comput.*, vol. 23, no. 5, pp. 5162–5178, May 2024.
- [36] X. Jiang et al., "Spatio-temporal routing, redundant coding and multipath scheduling for deterministic satellite network transmission," *IEEE Trans. Commun.*, vol. 71, no. 5, pp. 2860–2875, May 2023.
- [37] T. Li and Y. Cai, "Joint routing and scheduling for deterministic networking: A segment routing approach," in *Proc. IEEE 23rd Int. Conf. High Perform. Switching Routing*, 2022, pp. 189–194.
- [38] G. Peng, S. Wang, Z. Li, T. Huang, and C. Yuan, "Deterministic cognition: Cross-domain flow scheduling for time-sensitive networks," *IEEE Trans. Cogn. Commun. Netw.*, vol. 10, no. 4, pp. 1481–1495, Aug. 2024.
- [39] F. Wang, D. Wu, W. He, Z. Li, Q. Zhang, and H. Yao, "CPF: Bridging time-sensitive networks into large-scale LEO satellite networks," in *Proc. Int. Wireless Commun. Mobile Comput.*, 2023, pp. 1–6.
- [40] H. Yu, T. Taleb, K. Samdanis, and J. Song, "Toward supporting holographic services over deterministic 6G integrated terrestrial and non-terrestrial networks," *IEEE Netw.*, vol. 38, no. 1, pp. 262–271, Jan. 2024.
- [41] Y. Huang, X. Jiang, S. Chen, F. Yang, and J. Yang, "Pheromone incentivized intelligent multipath traffic scheduling approach for LEO satellite networks," *IEEE Trans. Wireless Commun.*, vol. 21, no. 8, pp. 5889–5902, Aug. 2022.
- [42] A. Guidotti et al., "Architectures and key technical challenges for 5G systems incorporating satellites," *IEEE Trans. Veh. Technol.*, vol. 68, no. 3, pp. 2624–2639, Mar. 2019.
- [43] M. Marchese, F. Patrone, and M. Cello, "DTN-based nanosatellite architecture and hot spot selection algorithm for remote areas connection," *IEEE Trans. Veh. Technol.*, vol. 67, no. 1, pp. 689–702, Jan. 2018.
- [44] F. D. Raverta, J. A. Fraire, P. G. Madoery, R. A. Demasi, J. M. Finochietto, and P. R. D'argenio, "Routing in delay-tolerant networks under uncertain contact plans," *Ad Hoc Netw.*, vol. 123, 2021, Art. no. 102663.
- [45] W. Zhang, D. Yang, C. Zhang, Q. Ye, H. Zhang, and X. Shen, "(Com)2Net: A novel communication and computation integrated network architecture," *IEEE Netw.*, vol. 38, no. 2, pp. 35–44, Mar. 2024.
- [46] L. Cheng et al., "Network-aware locality scheduling for distributed data operators in data centers," *IEEE Trans. Parallel Distrib. Syst.*, vol. 32, no. 6, pp. 1494–1510, Jun. 2021.
- [47] V. Niazmand and Q. Ye, "Joint task offloading, DNN pruning, and computing resource allocation for fault detection with dynamic constraints in Industrial IoT," *IEEE Trans. Cogn. Commun. Netw.*, early access, Jan. 14, 2025, doi: [10.1109/TCCN.2025.3529688](https://doi.org/10.1109/TCCN.2025.3529688).
- [48] M. Kim, J. Jang, Y. Choi, and H. J. Yang, "Distributed task offloading and resource allocation for latency minimization in mobile edge computing networks," *IEEE Trans. Mobile Comput.*, vol. 23, no. 12, pp. 15149–15166, Dec. 2024.
- [49] Q. He et al., "Routing optimization with deep reinforcement learning in knowledge defined networking," *IEEE Trans. Mobile Comput.*, vol. 23, no. 2, pp. 1444–1455, Feb. 2024.
- [50] J. Ren et al., "Toward deterministic wide-area networks via deadline-aware routing and scheduling," *IEEE Trans. Netw.*, early access, Mar. 24, 2025, doi: [10.1109/TON.2025.3546678](https://doi.org/10.1109/TON.2025.3546678).
- [51] W. Fan, X. Liu, H. Yuan, N. Li, and Y. Liu, "Time-slotted task offloading and resource allocation for cloud-edge-end cooperative computing networks," *IEEE Trans. Mobile Comput.*, vol. 23, no. 8, pp. 8225–8241, Aug. 2024.
- [52] T. Wang, J. Zhao, H. Leung, and W. Wang, "A condition knowledge representation and feedback learning framework for dynamic optimization of integrated energy systems," *IEEE Trans. Cybern.*, vol. 54, no. 5, pp. 2880–2890, May 2024.
- [53] W. Tan and B. Wu, "Long-distance deterministic transmission among TSN networks: Converging CQF and DIP," in *Proc. IEEE 29th Int. Conf. Netw. Protoc.*, 2021, pp. 1–6.



**Weiting Zhang** (Member, IEEE) received the PhD degree in communication and information systems from Beijing Jiaotong University, Beijing, China, in 2021. From November 2019 to November 2020, he was a visiting PhD student with the Department of Electrical and Computer Engineering, University of Waterloo, Canada. Starting from December 2021, he works as an associate professor with the School of Electronic and Information Engineering, Beijing Jiaotong University. His research interests include Industrial Internet of Things, deterministic networks, edge intelligence, and machine learning for network optimization.



**Peixi Liao** received the BS degree in communication engineering from Beijing Jiaotong University, Beijing, China, in 2022. She is currently working toward the MS degree in information and communication engineering with Jiaotong University, Beijing. Her research interests include satellite-terrestrial integrated network, deterministic networks, and computing and networking integration.



**Shiwen Mao** (Fellow, IEEE) is a professor and Earle C. Williams Eminent scholar, and director of the Wireless Engineering Research and Education Center, Auburn University. His research interests include wireless networks, multimedia communications, and smart grid. He is a distinguished lecturer of the IEEE Communications Society (ComSoc, 2021-2025), IEEE Council of RFID (2021-2023), and IEEE Vehicular Technology Society (VTS, 2014-2018), and a distinguished speaker of IEEE VTS (2018-2021). He is the editor in-chief of *IEEE Transactions on Cognitive Communications and Networking*. He was the general chair of IEEE INFOCOM 2022, a TPC chair of IEEE INFOCOM 2018, and a TPC vice-chair of IEEE GLOBECOM 2022. He received the IEEE ComSoc MMTTC Outstanding Researcher Award in 2023, the SEC (Southeastern Conference) 2023 Faculty Achievement Award for Auburn, the IEEE ComSoc TC-CSR Distinguished Technical Achievement Award in 2019, the Auburn University Creative Research & Scholarship Award in 2018, and the NSF CAREER Award in 2010, and several service awards from IEEE ComSoc. He is a co-recipient of the 2022 Best Journal Paper Award of IEEE ComSoc eHealth Technical Committee, the 2021 Best Paper Award of Elsevier/KeAi Digital Communications and Networks Journal, the 2021 IEEE Internet of Things Journal Best Paper Award, the 2021 IEEE Communications Society Outstanding Paper Award, the IEEE Vehicular Technology Society 2020 Jack Neubauer Memorial Award, the 2018 Best Journal Paper Award and the 2017 Best Conference Paper Award from IEEE ComSoc MMTTC, and the 2004 IEEE Communications Society Leonard G. Abraham Prize in the Field of Communications Systems. He is a co-recipient of the Best Paper Awards from GLOBECOM 2023 (two), 2019, 2016, and 2015, IEEE ICC 2022 and 2013, and IEEE WCNC 2015, and the Best Demo Awards from IEEE INFOCOM 2022, and IEEE SECON 2017.



**Dong Yang** (Member, IEEE) received the PhD degree in communication engineering from the School of Electronics and Information Engineering, Beijing Jiaotong University, China, in 2008. From March 2009 to July 2010, he was a post-doctoral researcher with Jönköping University and ABB Corporate Research, Sweden, where he participated in the standardization and innovation of industrial wireless sensor network. He is currently a full professor in communication engineering and the director of the Intelligent Industry Network Research Institute, Beijing Jiaotong University. His current research interests include network architecture, the Internet of Things, wireless sensor networks, and data driven network resource management. He has authored or coauthored more than 70 scientific publications in the field of network and communication technologies. More than 20 of his invention patents were licensed to ZTE. He has served as the co-chair for IEEE INFOCOM 2023 Workshop PerAI-6G, the session chair for IEEE ICCT 2022, and a TPC member for IEEE MetaCom 2023. He has been serving as an associate editor of *IEEE Transactions on Mobile Computing* and an executive editor of *Transactions on Emerging Telecommunications Technologies* (Wiley). He has served as the guest editor of *IEEE Transaction on Industrial Informatics* in 2021.



**Qiang (John) Ye** (Senior Member, IEEE) received the PhD degree in electrical and computer engineering from the University of Waterloo, Canada, in 2016. Since September 2023, he has been an assistant professor with the Department of Electrical and Software Engineering, Schulich School of Engineering, University of Calgary, Canada. Before joining UCalgary, he worked as an assistant professor with the Memorial University of Newfoundland, Canada, from 2021 to 2023, and with the Minnesota State University, Mankato, USA, from 2019 to 2021. He was with the Department of Electrical and Computer Engineering, University of Waterloo, as a post-doctoral fellow and then a research associate, from 2016 to 2019. He has published around 80 research papers in top-ranked journals and conference proceedings. He is/was a general, publication, publicity, TPC, or symposium co-chair for different reputable international conferences and workshops (e.g., IEEE INFOCOM, GLOBECOM, VTC, ICCC, ICCT, WISEE, SWC). He also serves/served as the IEEE Vehicular Technology Society (VTS) Region 7 Chapter coordinator in 2024, the IEEE Communications Society (ComSoc) Southern Alberta Chapter vice chair from 2024, and the VTS Regions 1-7 Chapters coordinator from 2022 to 2023. He is the leading co-chair of a special interest group (SIG) in the IEEE ComSoc - Internet of Things, Ad Hoc & Sensor Networks (IoT-AHSN) Technical Committee. He serves as an associate editor of the prestigious IEEE journals, such as the *IEEE Internet of Things Journal*, *IEEE Transactions on Vehicular Technology*, *IEEE Transactions on Cognitive Communications and Networking*, and *IEEE Open Journal of the Communications Society*. He received the Best Paper Award in the IEEE/CIC ICCC in 2024 and the IEEE Transactions on Cognitive Communications and Networking Exemplary Editor Award in 2023. He received the Early Career Research Excellence Award, Schulich School of Engineering, University of Calgary, in 2024. He has been selected as an IEEE ComSoc distinguished lecturer for the class of 2025–2026.



**Hongke Zhang** (Fellow, IEEE) received the MSc and PhD degrees in electrical and communication systems from the University of Electronic Science and Technology of China, Chengdu, China, in 1988 and 1992, respectively. From 1992 to 1994, he was a post-doctoral researcher with Beijing Jiaotong University, Beijing, China, where he is currently a professor with the School of Electronic and Information Engineering and the director of the National Engineering Laboratory on Next Generation Internet Technologies. His research has resulted in many articles, books, patents, systems, and equipment in the areas of communications and computer networks. He is the author of more than ten books and the holder of more than 70 patents. He is the chief scientist with the National Basic Research Program of China (973 Program) and has also served on the editorial boards for several international journals.